Published in final edited form as:
J Med Chem. 2008 October 9; 51(19): 6110–6120. doi:10.1021/jm8005788.

Discovery of inhibitors of *Escherichia coli* methionine aminopeptidase with the Fe(II)-form selectivity and antibacterial activity†

Wen-Long Wang[1], **Sergio C. Chai**[1], **Min Huang**[2], **Hong-Zhen He**[1], **Thomas D. Hurley**[1], and **Qi-Zhuang Ye**[1,2,*]

[1]Department of Biochemistry and Molecular Biology, Indiana University School of Medicine, Indianapolis, Indiana 46202

[2]High Throughput Screening Laboratory, University of Kansas, Lawrence, Kansas 66045

Abstract

Methionine aminopeptidase (MetAP) is a promising target to develop novel antibiotics, because all bacteria express MetAP from a single gene that carries out the essential function of removing N-terminal methionine from nascent proteins. Divalent metal ions play a critical role in the catalysis, and there is an urgent need to define the actual metal used by MetAP in bacterial cells. By high throughput screening, we identified a novel class of catechol-containing MetAP inhibitors that display selectivity for the Fe(II)-form of MetAP. X-ray structure revealed that the inhibitor binds to MetAP at the active site with the catechol coordinating to the metal ions. Importantly, some of the inhibitors showed antibacterial activity at low micromolar concentration on Gram-positive and Gram-negative bacteria. Our data indicate that Fe(II) is the likely metal used by MetAP in the cellular environment, and MetAP inhibitors need to inhibit this metalloform of MetAP effectively to be therapeutically useful.

Introduction

Although methionine aminopeptidase (MetAP) is considered as a promising target for development of new antibiotics with novel mechanism of action [1, 2], current small molecule MetAP inhibitors with high potencies on purified enzymes failed to show any significant antibacterial activity [3–5]. This is puzzling because MetAP carries out removal of the initiator methionine residue from newly synthesized proteins, and this removal is critical for activation, distribution and stability of many proteins [1]. MetAP in bacteria is coded by a single gene and is essential for bacterial survival, because deletion of this gene in *Escherichia coli* or *Salmonella typhimurium* was shown to be lethal [6, 7]. Divalent metal ions play a key role in the peptide hydrolysis catalyzed by MetAP, and purified apoenzyme of MetAP can be activated by several divalent metals, including Co(II), Mn(II), and Fe(II) [8, 9]. Initially, MetAP was believed to be a Co(II) enzyme, because Co(II) is among the best activators and early X-ray structures of MetAP all contain two Co(II) ions at the active site [10]. Most of the currently known MetAP inhibitors were discovered and characterized with MetAP in the Co(II)-form. However, we showed that inhibitors of the Co(II)-form may or may not inhibit other metalloforms of

†Coordinates and structure factors for *E. coli* methionine aminopeptidase complexed to **22** have been deposited in the Protein Data Bank under the access code 3D27.

*Author to whom correspondence may be sent: Department of Biochemistry and Molecular Biology, Indiana University School of Medicine, 635 Barnhill Drive, Indianapolis, Indiana 46202. Phone, 317-278-0304. E-Mail, yeq@iupui.edu.

MetAP [9, 11]. Thus, although there are many factors that an in vitro active compound may be inactive in vivo, such as absorption or metabolism, one explanation for the lack of antibacterial activities may be a disparity between the metalloform tested using a purified enzyme and the one that is important in cells. Walker and Bradshaw [12] suggested Zn(II) as a possible physiologically relevant metal because activity of Zn(II) substituted MetAP from *Saccharomyces cerevisiae* increased 1.7 fold under physiological concentration of reduced glutathione, while that of Co(II) substitution became inactive under the same condition. However, Yang et al. [13] concluded that Zn(II) is not the physiologically relevant metal in human type II MetAP and attributed the stoichiometric amount of Zn(II) associated with the enzyme to the Zn(II) that binds on protein surfaces. D'souza et al. [8] suggested that *E. coli* MetAP is a Fe(II) enzyme based on combination of whole cell metal analysis, enzyme activity measurements, and studies of substrate binding constants. Mn(II) is also a candidate, because the Mn(II)-form of *E. coli* MetAP is catalytically competent [14], and Mn(II) was suggested to be the physiological metal for human type II MetAP [15].

In the process of creating research tools to define the actual metal used by MetAP in cells, we have previously discovered two distinct classes of novel nonpeptidic MetAP inhibitors (e.g., **1** and **2** in Fig. 1) by screening a diverse chemical library of small organic compounds; each has a unique structural scaffold and each comprises several potent inhibitors highly selective for either the Mn(II) or the Co(II)-form of *E. coli* MetAP [11]. Fe(II) is one of the best activators of MetAP besides Co(II) and the candidate metal for MetAP in *E. coli* cells [8]. Now, we report the discovery of a new class of small molecule MetAP inhibitors, such as **3** (Fig. 1), by high throughput screening that showed high selectivity toward the Fe(II)-form. Some of these inhibitors clearly showed antibacterial activity, suggesting that Fe(II) is likely the physiologically relevant metal for MetAP in *E. coli* cells, and maybe also in other bacterial cells.

Results and Discussion

Discovery of MetAP inhibitors with selectivity for the Fe(II)-form by high throughput screening

With no lead structures available for MetAP inhibitors that are selective for the Fe(II)-form, we turned to high throughput screening to identify such inhibitors with novel chemical structures. Activation of apoenzyme of *E. coli* MetAP by divalent metal ions is instantaneous [9], so that the screening was performed using purified apoenzyme with Fe(II) ion added immediately before monitoring hydrolysis of a fluorogenic substrate. The substrate Met-AMC is a methionine derivatized with 7-amino-4-methylcoumarin (AMC), and its hydrolysis produces AMC detectable by fluorescence [13]. Fe(II) is an excellent activator, while Fe(III) cannot activate MetAP. Oxidation of Fe(II) to Fe(III) during the initial 12 min of the reaction was noticeable but not significant, because increase in fluorescence was nearly linear during this period. The screening assay measured the rate of substrate hydrolysis by MetAP in the presence or absence of screening compounds in kinetic mode by monitoring the increase in fluorescence for 12 min. A total of 74,976 compounds were screened at a single final concentration of 6.25 μg/mL. This screening campaign generated high-quality data with z' factors [16] between 0.50 and 0.83 and their average at 0.67. Initial screening hits were further confirmed by determining their IC_{50} values using 6 serially diluted concentrations. Among confirmed hits is **3** with a catechol moiety. When **3** was characterized on the Co(II)-, Mn(II)- and Fe(II)-forms of *E. coli* MetAP, it showed low micromolar potency (13 μM) on the Fe(II)-form but showed no activity against the Co(II)-and Mn(II)-forms at the highest tested concentration of 100 μM (Table 1). Therefore, it has both significant inhibitory potency and considerable selectivity and represents an early lead structure for further development.

Metalloform-selective inhibitors are both valuable research tools to define the physiologically relevant metal for MetAP and useful lead compounds to develop novel antibacterial, antifungal and anticancer agents. Discovery of the new class of nonpeptidic inhibitors with unique selectivity toward the Fe(II)-form, once again, demonstrated the power of high throughput screening technology in identifying compounds with novel activities.

Requirement of a catechol moiety for the inhibitory activity

The lead structure of **3** can be broken down to the catechol moiety and the thiazole moiety. We initially prepared **4–10** by the route outlined in Scheme 1, in which we substituted the dihydroxyl group on the phenyl ring of **3** with hydroxyl, methoxyl, amino, nitro, acetylamido, and aminocarbonyl groups. We noticed that none of them showed enzyme inhibition on the three metalloforms tested (up to 100 μM). This result underscores importance of the catechol moiety for activity, and the catechol possibly functions as a metal chelating group for the active site metal ions. The chelation by the adjacent hydroxyls with the metal likely contributes greatly to its activity because separating the hydroxyls (**4**), removing one of the hydroxyls (**5**), blocking the hydroxyls (**6**), or replacement with amino, nitro and other groups (**7–10**) all voided the activity. These results indicated that the adjacent hydroxyl groups on the phenyl ring is essential for effective inhibition of the Fe(II)-form of MetAP.

Synthesis of thiazole and thiophene derivatives with a catechol moiety

To further understand the key structural scaffold, additional four thiazoles were designed, in which the catechol moiety is unchanged, while attachment of the thiazole moiety is varied, forming 2-phenylthiazole (**14**), 4-phenylthiazole (**11**) or 5-phenylthiazoles (**12**, **13**). The syntheses of **11**, **12** and **13**, and **14** are shown in Scheme 1, Scheme 2, and Scheme 3, respectively. In scheme 2, the Michael addition reaction occurred in the Darzens condensation of methyl dichloroacetate and **30** 17, and the resulted intermediate reacted with ethanethioamide to form 2-methylthiazole-4-carboxylate **31** 18. Hydrolysis of **31** gave **32**, followed by condensation with appropriate amines to afford **12a** and **13a**. Afterwards, the protective group of hydroxyls was removed to yield **12** and **13** (36%– 50% yield).

2-Phenylthiazole **14** was synthesized by the Suzuki coupling reaction as outlined in Scheme 3. Coupling of appropriate phenylboronic acid with corresponding halogenated thiazole yielded **14a**. The protective group of hydroxyls was removed by using BCl_3, yielding **14**.

Fifteen thiophene derivatives were also made and can be divided into 2-phenylthiophenes (**15–25**) or 3-phenylthiophenes (**26–29**) according to their attachment to the catechol moiety. Same Suzuki coupling was employed to make **15a–29a** 19. Removal of the protective groups of hydroxyls produced **15** and **16** by using BCl_3 or **17–29** by using BBr_3.

Inhibition of the Co(II)-, Mn(II)- or Fe(II)-form of *E. coli* MetAP

We tested the synthesized phenylthiazoles and phenylthiophenes on the Co(II)-, Mn(II)- and Fe(II)-forms of *E. coli* MetAP to reveal the structural elements that are important in inhibitory potency and metalloform selectivity. All thiazoles **11–14**, as well as the lead **3**, showed low micromolar potency on the Fe(II)-form of MetAP and inactivity on the Co(II)- or Mn(II)-form, displaying considerable selectivity towards the Fe(II)-form (Table 1). It is interesting to note that although these thiazoles fused to the catechol with different positions (position 4 of the thiazole ring for **3** and **11**, position 5 for **12** and **13**, and position 2 for **14**), neither potency nor selectivity was significantly affected.

Generally speaking, phenylthiophenes inhibited the Fe(II)-form of *E. coli* MetAP effectively with low micromolar potency. Some of the thiophenes, such as **17**, **25**, and **29**, also displayed low micromolar potency on the Co(II)- and Mn(II)-forms, indicating that their selectivity for

the Fe(II)-form was reduced. Nevertheless, **15** and **27** still showed good selectivity for the Fe (II)-form.

It is noticeable that all substitutions on the thiazole and thiophene rings were well tolerated for inhibition of the Fe(II)-form. MetAP as an exopeptidase has a shallow and mostly hydrophobic substrate-binding pocket with the catalytic metal sitting at the bottom of the pocket [10]. Consistent with importance of the catechol moiety in the inhibitory activity and metalloform selectivity, a binding model is conceivable that the dihydroxyl group of catechol interacts with the catalytic metal ions, leaving the substituents on the thiazole or thiophene ring pointing towards the opening of the pocket. This arrangement for the substituents explains the observed inhibitory activity.

X-ray structure of *E. coli* MetAP in complex with inhibitor 22

To elucidate the exact binding mode of these newly discovered inhibitors on MetAP enzymes, an X-ray structure of the enzyme-inhibitor complex is desirable. However, the Fe(II)-form MetAP poses a significant challenge in crystallization due to the ease with which the ferrous ions oxidized and yielded undesirable precipitates of the protein in our initial crystallization experiments. To circumvent this problem, we attempted crystallization using the Mn(II)-form MetAP with several of these newly discovered inhibitors because we believe that the inhibitors bind to the two metalloforms of MetAP in the same mode. We succeeded in obtaining diffraction-quality crystals of *E. coli* MetAP in complex with **22** in the Mn(II)-form and solved the structure to 2.2 Å resolution (Fig. 2, Table 2).

Consistent with the above prediction of the binding mode based on observed inhibitory activities of these unique inhibitors, inhibitor **22** indeed binds to MetAP at the substrate binding pocket with its hydroxyl groups of the catechol moiety chelating with two metal ions at the dinuclear metal site. One hydroxyl oxygen interacts only with the metal labeled as Mn1, which is the tighter bound metal ion [14], while the other hydroxyl oxygen interacts with both Mn1 and Mn2 in a monodentate bridging mode. The distance between the two metal ions is 3.38Å, and both metal ions exhibit octahedral coordination geometry. A strictly conserved water molecule (w1) found in many MetAP structures is also coordinated to Mn2. The phenyl ring of the inhibitor is not coplanar with the five-membered thiophene ring, probably to accommodate the steric bulk of an ortho-substituted ethyl group. The ethyl group is pointing towards inside of the pocket. This is consistent with our previous findings that small and non-polar side chains are tolerated in this pocket [20]. The non-coplanar arrangement makes the conformation of the five-membered ring more flexible and provides one option of accommodating larger and more polar groups by rotating the bond joining the catechol and thiazole or thiophene to position the substituent towards the mouth of this binding pocket (Fig. 2B). This explains the tolerance of functional groups with different sizes on the five-membered rings.

The Fe(II)-form selectivity

It is intriguing how these inhibitors achieve metalloform selectivity, considering that X-ray structures of different metalloforms of MetAP are very similar overall and at the active site [11, 21]. Comparing this structure (pdb code 3D27) with the previous MetAP structure in complex with the Mn(II)-form selective inhibitor **2** (pdb code 1XNZ), they are very similar because superimposition of the two structures gives a root mean square deviation (rmsd) value of 0.23Å for the backbone atoms of residues 4–256 (Fig. 2B). With overall similarity of the two structures, the major difference is the coordination of the two inhibitors to the metal ions. The Mn(II)-form selective inhibitor **2** coordinates with the metal ions using its carboxyl oxygens, while the Fe(II)-form selective inhibitor **22** uses two oxygens from the catechol for the coordination. It is likely that electronic properties and the geometry of the two catechol oxygens

in **22** specifically satisfy the requirements for coordination to the Fe(II) ions, leading to the observed selectivity for the Fe(II)-form of MetAP.

The large number of compounds in the screening library were selected for structural diversity and drug-like properties. From these compounds with diverse structures, this screening campaign by chance identified compounds with a catechol moiety as inhibitors of the Fe(II)-form MetAP. However, this is not surprising retrospectively, because the catechol moiety is known for its affinity for Fe(II) and Fe(III) ions [22]. Microbes use catechol-containing siderophores, such as enterobactin, for iron transport [23]. Analysis of the structures of the active (**3**, **11–29**) and inactive (**4–10**) compounds confirms the importance of the catechol moiety in their inhibitory activity. The two phenolic hydroxyl groups must be in adjacent positions, which is consistent with observation in the crystal structure that the two groups directly coordinate with the metal ions.

Inhibition of growth of *E. coli* and *Bacillus* bacterial strains

MetAP is an essential enzyme in bacteria [6, 7], and MetAP in *E. coli* was suggested to be a Fe (II) enzyme [8]. Conceivably, the Fe(II)-form selective MetAP inhibitors will inhibit growth of bacterial cells. We selected two *E. coli* strains (Gram-negative) and two *Bacillus* strains (Gram-positive) for testing these MetAP inhibitors for antibacterial activity. While we did not see any antibacterial activity from the Co(II)- or Mn(II)-form selective inhibitors, such as **1** and **2**, at the highest concentration tested (1 mM), we observed for the first time definite inhibition of cell growth at low micromolar concentrations of MetAP inhibitors (Table 1).

Both *E. coli* AS19 [24] and D22 [25] strains have genetic mutations so that their cell membranes are weakened in different ways for better penetration by small organic molecules. The two *Bacillus* strains are Gram-positive and believed to be more permeable to small molecules, and they are both wild type strains. Initial inhibitory activity on growth of *E. coli* D22 seen by **3** at 5.6 μM was encouraging. However, it inhibited growth of other three strains only modestly, and other thiazoles **11–14** did not improve the activity on growth inhibition, although they maintained potency and selectivity for the Fe(II)-form MetAP. With both inhibition of enzymatic activity on purified proteins and inhibition of bacterial growth as guidance, a series of thiophene derivatives were made and tested. Clearly, most of the thiophene derivatives showed much improved antibacterial activity, and the activity was seen on all four strains tested. Several of the thiophene derivatives have much improved antibacterial activity over the initial lead **3**. The thiophene **28** is among the best with IC_{50} values of 6.1 μM for *E. coli* AS19, 7.3 μM for *E. coli* D22, 6.0 μM for *B. subtilis*, and 5.0 μM for *B. megaterium*.

Inhibition between *E. coli* AS19 and D22 strains showed bigger variations than that between two *Bacillus* strains. For example, **3**, **17**, and **26** had much better potency on *E. coli* D22 than on *E. coli* AS19, and **15**, **16**, **19**, and **23** showed just the opposite. This observation may reflect the different mutations of *E. coli* AS19 and D22 strains, which render their membranes with different permeabilities to different inhibitors. The amide derivatives **12**, **13**, **15** and **16** all showed reduced cellular activity. The fact that they all inhibited the Fe(II)-form MetAP effectively indicates their possible difficulties in penetrating bacterial cell membranes due to the amide structure.

These bacterial strains provided the platforms to correlate inhibition of enzymatic activity and inhibition of bacterial cell growth. To evaluate the potential as an antibacterial therapeutics, we also tested two of these inhibitors on wild type *E. coli* strain ATCC25922, where its membrane is tougher to penetrate. We observed reduced but still measurable antibacterial activity with IC_{50} at 281 μM and 179 μM for **3** and **21**, respectively. This result confirms the potential to develop MetAP inhibitors with effective inhibition of the Fe(II)-form MetAP as novel antibacterial drugs.

Bacterial MetAP enzymes belong to type I MetAP and are homologous to human type I MetAP in sequence. Although human type II MetAP was suggested to be a Mn(II) enzyme [15], the native metal for human type I MetAP is undefined. For therapeutic applications, MetAP inhibitors should block the activity of bacterial enzymes but spare the human counterparts. The metalloform-selective inhibition is a feature that could potentially be utilized to achieve such selectivity.

Conclusion

By high throughput screening, we discovered a novel class of inhibitors with potency and selectivity for the Fe(II)-form of *E. coli* MetAP. Structural modifications of the initial lead structure **3** and X-ray structural analysis of MetAP complexed with inhibitor **22** confirmed the requirement of a catechol moiety for the inhibitory activity and revealed their binding mode on the enzyme. Thiazole derivatives showed both excellent potency and selectivity of the Fe (II)-form on the purified enzyme and displayed considerable activity on growth inhibition of bacterial cells. Thiophene derivatives maintained effective inhibition of the Fe(II)-form of *E. coli* MetAP and some of them showed much improved inhibition on growth of all four tested Gram-positive and Gram-negative bacterial strains. The correlation between inhibition of the Fe(II)-form MetAP and antibacterial activity indicates that the Fe(II)-form is likely the physiologically relevant metalloform of MetAP and these unique inhibitors have potential to be developed as new antibiotics with novel mechanism of action.

Experimental Section

General Methods

All chemicals were reagent-grade or better and used as purchased. All reactions were performed under an inert atmosphere of dry argon or nitrogen using distilled dry solvents, and most reactions were not optimized. Where NMR data are presented, ^{1}H spectra were obtained on either a Bruker Avance II 500 (500 MHz) or Varian Gemini 2000 (200 MHz), and ^{13}C spectra were obtained on a Bruker Avance II 500 (125 MHz). Chemical shifts were reported in δ (ppm) using δ 7.26 signal of $CDCl_3$ (^{1}H NMR), δ 77.23 signal of $CDCl_3$ (^{13}C NMR), δ 3.31 signal of CD_3OD (^{1}H NMR), δ 49.15 signal of CD_3OD (^{13}C NMR), or δ 2.50 signal of DMSO-*d6* (^{1}H NMR) as the internal standard. High-resolution MS data were obtained on either a Thermo Finnigan MAT-95 XP or a Waters/Micromass LCT. LC-MS analyses were conducted using an Agilent system, consisting of a 1100 series HPLC connected to a diode array detector and a 1946D mass spectrometer configured for positive-ion/negative-ion electro-spray ionization. System A: column, Zorbax SB-C18, 4.6×150 mm, 5 μm; flow rate, 1.0 mL/min; UV wavelength, 254 nm; temperature, ambient; injection volume, 10 μL; A linear gradient using water with 0.1% TFA (solvent A) and acetonitrile with 0.1% TFA (solvent B); t = 0 min, 30% B, t = 15 min 100% B, t = 18 min, 100% B. System B: column, Supelco Ascentis C18, 4.6×150 mm, 5 μm; flow rate, 1.0 mL/min; UV wavelength, 254 nm; temperature, ambient; injection volume, 10 μL; A linear gradient using water with 0.1% TFA (solvent A) and methanol with 0.1% TFA (solvent B); t = 0 min, 25% B, t = 12 min 100% B, t = 17 min, 100% B.

The reaction mixture was generally poured into water, and the separated aqueous phase was then thoroughly extracted with the specified solvent. After the mixture was washed with 10% aqueous HCl and/or $NaHCO_3$ (if required), water and brine, the combined organic phases were dried over anhydrous Na_2SO_4 or $MgSO_4$ and then filtered and concentrated under reduced pressure to yield the crude reaction product. Separations by column chromatography were carried out using Dynamic Adsorbents Silica Flash 60A (40–63μ). Concentration and evaporation refer to removal of volatile material under reduced pressure on a Buchi rotavapor.

General Procedures

Procedure A—General Procedures for the Preparation of **5–10**. To a stirred solution of N-(4-(2-chloroacetyl)-2-nitrophenyl)acetamide (1.283 g, 5 mmol) in EtOH (30 mL) was added thioactamide (6 mmol) and the mixture refluxed for 2 h. After cooling of the solvent, the precipitate was collected to yield **7** (1.18 g, 85%). TLC (SiO_2, 30% EtOAc/Hexane): R_f = 0.32. ^{1}H NMR (DMSO-*d6*, 200 MHz) δ 2.10 (s, 3H), 2.75 (s, 3H), 7.72 (d, *J* = 8.4 Hz, 1H), 8.14 (s, 1H), 8.24 (dd, *J* = 8.4 Hz, 2.2 Hz, 1H), 8.46 (d, *J* = 1.8 Hz, 1H), 10.33 (s, 1H). MS (ESI(+)) *m/z* 278 $[M + H]^+$.

A solution of 6N HCl (3 mL) was added to a stirred suspension of 7 (554 mg, 2 mmol) in ethanol (3 mL) and the resulting mixture was refluxed for 4 h. The solvent was then vacuum-evaporated and the resulting aqueous layer was extracted with EtOAc (100 mL). The organic extracts were washed with saturated $NaHCO_3$ solution, brine, dried ($MgSO_4$) and concentrated to dryness. The residue was purified by column chromagraphy on silica gel, using a mixture of CH_2Cl_2: MeOH (100:3) as the eluent, to provide **8** (235 mg, 50%). ^{1}H NMR (DMSO-*d6*, 200 MHz) δ 2.71 (s, 3H), 5.91 (br, 2H), 7.09 (d, *J* = 8.8 Hz, 1H), 7.81 (s, 1H), 7.96 (dd, *J* = 8.8 Hz, 2.2 Hz, 1H), 8.54 (d, *J* = 1.8 Hz, 1H). MS (ESI(+)) *m/z* 236 $[M + H]^+$.

A solution of the nitro derivative **8** (200mg, 0.85 mmol) was hydrogenated in the presence of 10% Pd/C (30 mg) at room temperature for 4 h. The mixture was then filtered through a Celite pad, and the filtrate was evaporated to dryness to afford the amine **9** (596 mg, 70%). TLC (SiO_2, 5% MeOH/CH_2Cl_2): R_f = 0.32. ^{1}H NMR (CD_3OD, 500 MHz) δ 2.72 (s, 3H), 6.72 (d, *J* = 8.0 Hz, 1H), 7.12 (dd, *J* = 8.0 Hz, 2.0 Hz, 1H), 7.20 (d, *J* = 2.0 Hz, 1H), 7.28 (s, 1H). MS (ESI(+)) *m/z* 206 $[M + H]^+$.

4-(2-methylthiazol-4-yl)benzene-1,3-diol (4): This compound was prepared by a procedure analogous to that of compound **7**, Yield: 80%; TLC (SiO_2, 30% EtOAc/Hexane): R_f = 0.33. ^{1}H NMR (DMSO-*d6*, 500 MHz) δ 2.72 (s, 3H), 6.31(dd, *J* = 8.5 Hz, 4.0 Hz, 1H), 6.33 (d, *J* = 4.0 Hz, 1H), 7.72 (d, *J* = 8.5 Hz, 1H), 7.73 (s, 1H), 9.51 (s, 1H), 10.93 (s, 1H). MS (ESI (+)) *m/z* 208 $[M + H]^+$.

3-(2-methylthiazol-4-yl)phenol (5): This compound was prepared by a procedure analogous to that of compound **7**, Yield: 85%; TLC (SiO_2, 10% EtOAc/Hexane): R_f = 0.12. ^{1}H NMR ($CDCl_3$, 500 MHz) δ 2.77 (s, 3H), 5.69 (s, 1H), 6.81 (m, 1H), 7.26 (m, 2H), 7.38 (m, 2H). MS (ESI(+)) *m/z* 192 $[M + H]^+$.

4-(3,4-dimethoxyphenyl)-2-methylthiazole (6): This compound was prepared by a procedure analogous to that of compound **7**, Yield: 87%; TLC (SiO_2, 20% EtOAc/Hexane): R_f = 0.15. ^{1}H NMR ($CDCl_3$, 500 MHz) δ 2.77 (s, 3H), 3.92 (s, 3H), 3.97 (s, 3H), 6.90 (d, *J* = 8.5 Hz, 1H), 7.19 (s, 1H), 7.40 (dd, *J* = 8.0 Hz, 2.0 Hz, 1H), 7.45 (d, *J* = 2.0 Hz, 1H). MS (ESI(+)) *m/z* 236 $[M + H]^+$.

2-hydroxy-5-(2-methylthiazol-4-yl)benzamide (10): This compound was prepared by a procedure analogous to that of compound **7**, Yield: 90%; TLC (SiO_2, 30% EtOAc/Hexane): R_f = 0.25. ^{1}H NMR (DMSO-*d6*, 200 MHz) δ 2.48 (s, 3H), 6.71 (d, *J* = 8.4 Hz, 1H), 7.52 (s, 1H), 7.74 (dd, *J* = 8.4 Hz, 2.2 Hz, 1H), 8.17 (d, *J* = 2.2 Hz, 1H); MS (ESI(+)) *m/z* 235 $[M + H]^+$.

4-(2-aminothiazol-4-yl)benzene-1,2-diol (11): This compound was prepared by a procedure analogous to that of compound **7**, Yield: 90%; TLC (SiO_2, 60% EtOAc/Hexane): R_f = 0.15. ^{1}H NMR (CD_3OD, 500 MHz) δ 6.78 (s, 1H), 6.86 (d, *J* = 8.5 Hz, 1H), 6.98 (dd, *J* = 8.5

Hz, 2.0 Hz, 1 H), 7.05 (d, J = 2.0 Hz, 1H); ^{13}C NMR (CD_3OD, 125 MHz) δ 100.64, 114.34, 117.01, 119.26, 121.33, 141.16, 147.33, 148.88, 172.63.

Procedure B—General procedure for the preparation of p**12–13**. A solution prepared from Na (40.3 mmol, 1 g) and MeOH (20 mL) was added to a stirred solution of 3,4-bis(benzyloxy) benzaldehyde (31mmol, 9.9 g) and methyl dichloroacetate (37.2 mmol, 3.8 mL) in THF (50 mL) at 0°C. After stirring for 15 min, the solution was warmed to room temperature and stirred for 3 h. The reaction was poured into brine under ice-bath cooling and extracted with ethyl acetate. The organic layer was dried over anhydrous sodium sulfate, and evaporated under reduced pressure. Methanol (20 mL), ethanethioamide (35 mmol, 2.66 g) were added to the residue and refluxed for 3 h. To above reaction mixture, methanesulfonic acid (35 mmol, 2.43 mL) was added and the reaction mixture was continuously refluxed overnight. The mixture was cooled to room temperature and the resulting precipitate **31** (8.2 g, 43%) was collected by filtration. MS (ESI(+)) *m/z* 447 $[M + H]^+$.

Lithium hydroxide monohydrate (0.8 mmol, 35 mg) was added to a stirred solution of **31** (0.39 mmol, 200 mg) in MeOH/H_2O (0.75 mL / 0.25 mL) at 0°C and stirred for 1 h with gradual warming to room temperature. TLC monitoring showed complete consumption of starting material. The solvents were removed and the residue was partitioned between EtOAc (10 mL) and H_2O (5 mL). The organic phase was separated and the aqueous phase was acidified to pH = 2 with aqueous HCl (1 M) and then extracted with EtOAc. The combined organic phases were then processed in the usual way to **32** (190 mg). To the mixture of compound **32** (0.3 mmol, 150 mg), DMAP (0.12 mmol, 16 mg), EDC (0.45 mmol, 87 mg) and 4Å molecular sieves in appropriate DCM at room temperature were added to cyclopropyl amine (0.3 mmol, 38 μL), and the result mixture was stirred for 8 hours at room temperature. The reaction mixture was diluted with EtOAc (50 mL) and H_2O (20 mL). The aqueous phase was extracted with EtOAc. The combined organic phases were then processed in the usual way and chromatographed (1/1 petroleum ether/EtOAc) to yield **12a** (100 mg, 63%). Then the intermediate **12a** (0.19 mmol, 100 mg) was dissolved in CH_2Cl_2 at −80°C, following 1 M BCl_3 (1 mL) in CH_2Cl_2 added dropwise with stirring. Stirring continued at −80°C for 3 hr and room temperature for 10 hr. The reaction was terminated by careful dropwise addition of water at 0°C, and the mixture was abstracted by EtOAc. The combined organic layers were washed with water and brine and dried with anhydrous magnesium sulfate. The resulting residue was chromatographed on silica gel (2/1 EtOAc/Hexane) to afford **12** (20mg, 36%). ^{1}H NMR (CD_3OD, 200 MHz) δ 0.56 (m, 2H), 0.77 (m, 2H), 2.64 (s, 3H), 2.72 (m, 1H), 6.82 (2H), 6.97 (d, J = 2.2 Hz, 1H); ^{13}C NMR (CD_3OD, 125 MHz) δ 6.56, 18.58, 23.45, 116.11, 117.97, 122.69, 122.97, 142.43, 143.66, 146.14, 147.61, 164.95, 166.50. MS (ESI(+)) *m/z* 291 $[M + H]^+$; HRMS (CI) *m/z* 290.0726 (calcd for $C_{14}H_{14}N_2O_3S$ 290.0725).

5-(3,4-dihydroxyphenyl)-N-isopropyl-2-methylthiazole-4-carboxamide (13): was obtained from **32** according to procedure for **12** (two step 31%); TLC (SiO_2, 65% EtOAc/ Hexane): R_f = 0.43. ^{1}H NMR (CD_3OD, 500 MHz) δ 1.20 (d, J = 6.5 Hz, 3H), 1.25 (d, J = 7.5 Hz, 3H), 2.68 (s, 3H), 4.10 (m, 1H), 6.79 (d, J = 8.0 Hz, 1H), 6.86 (dd, J = 8.0 Hz, 2.0 Hz, 1 H), 6.98 (d, J = 2.0 Hz, 1H); ^{13}C NMR (CD_3OD, 125 MHz) δ 18.75, 22.65, 42.83, 116.32, 118.11, 122.82, 123.19, 143.10, 143.34, 146.35, 147.75, 164.34, 165.14. HRMS (CI) *m/z* 292.0883 (calcd for $C_{14}H_{16}N_2O_3S$ 292.0882).

Procedure C—General procedure for the preparation of **14–29**. To a solution of 2-bromothiazole (0.9 mmol, 146 mg), 3,4-bisbenzyloxyphenyl boronic acid [26] (600 mg, 1.78 mmol), and tetrakis(triphenylphosphine)-palladium (0) (0.09 mmol, 104 mg) in DMF (15 mL) was added 2M aqueous Na_2CO_3 (6 mmol, 3 mL). The reaction mixture was stirred at 80°C for 15 h. The reaction was quenched with water (100 mL) and extracted with EtOAc (300 mL). The combined organic layers were washed with water and brine and dried with anhydrous

magnesium sulfate. The solvent was removed in vacuo. The resulting residue was chromatographed on silica gel (5% – 50% EtOAc/Hexane) to afford intermediates **14a**. Yield 67%. ^{1}H NMR ($CDCl_3$, 200 MHz) δ 5.22 (s, 2H), 5.24 (s, 2H), 6.97 (d, *J* = 8.4 Hz, 1H), 7.31–7.51 (12H), 7.66 (d, *J* = 1.8 Hz, 1H), 7.80 (d, *J* = 3.2 Hz, 1H). MS (ESI(+)) *m/z* 374 $[M+H]^+$.

Then the intermediate **14a** (0.5 mmol, 187 mg) was dissolved in CH_2Cl_2 (3 mL) at −80°C, following 1 M BCl_3 in CH_2Cl_2 (3 mL) added dropwise with stirring. Stirring continued at −80° C for 3 hr and room temperature for 5 hr. The reaction was terminated by careful dropwise addition of water (5 mL) at 0°C, and the mixture was abstracted by EtOAc (15 mL). The combined organic layers were then processed in usual way and chromatographed on silica gel (50% – 100% EtOAc/Hexane) to afford **14** (71mg, 73%). ^{1}H NMR (CD_3OD, 500 MHz) δ 6.98 (d, *J* = 8.0 Hz, 1H), 7.40 (d, *J* = 2.0 Hz, 1H), 7.41 (dd, *J* = 8.0 Hz, 2.0 Hz, 1H), 7.91 (d, *J* = 4.0 Hz, 1H), 8.10 (d, *J* = 3.5 Hz, 1H); ^{13}C NMR (CD_3OD, 125 MHz) δ 115.29, 117.57, 119.28, 122.04, 122.39, 135.52, 147.95, 153.16, 173.59; MS (ESI(−)) *m/z* 192 $[M-H]^-$.

2-(3,4-bis(benzyloxy)phenyl)-N-cyclopropylthiophene-3-carboxamide (15a): was obtained from 3,4-bisbenzyloxyphenyl boronic acid and 2-bromo-N-cyclopropylthiophene-3-carboxamide [27] according to the procedure described for **14a** in 55%. TLC (SiO_2, 50% EtOAc/Hexane): R_f = 0.21. ^{1}H NMR ($CDCl_3$, 500 MHz) δ 0.22 (m, 2H), 0.68 (m, 2H), 2.68 (m, 1H), 5.17 (s, 2H), 5.24 (s, 2H), 5.51 (brs, 1H), 6.98 (m, 2H), 7.06 (m, 1H), 7.21 (d, *J* = 5.5 Hz, 1H), 7.33 (m, 2H), 7.38 (m, 4H), 7.41 (d, *J* = 5.5 Hz, 1H), 7.47 (m, 4H).

N-cyclopropyl-2-(3,4-dihydroxyphenyl)thiophene-3-carboxamide (15): was obtained from **15a** according to the procedure described for **14** in 32%. TLC (SiO_2, 60% EtOAc/Hexane): R_f = 0.32. ^{1}H NMR (CD_3OD, 500 MHz) δ 0.42 (m, 2H), 0.69 (m, 2H), 2.71 (m, 1H), 6.79 (m, 2H), 6.88 (m, 1H), 7.16 (d, *J* = 5.5 Hz, 1H), 7.29 (d, *J* = 5.5 Hz, 1H); ^{13}C NMR (CD_3OD, 125 MHz) δ 6.51, 23.74, 116.60, 117.23, 121.85, 125.04, 125.91, 129.37, 133.67, 146.26, 146.65, 147.44, 170.08. MS (ESI(+)) *m/z* 276 $[M+H]^+$; HRMS (ESI(+)) m/z 276.0696 (calcd for $C_{14}H_{14}NO_3S$ 276.0694).

5-(3,4-bis(benzyloxy)phenyl)-N-cyclopropylthiophene-2-carboxamide (16a): was obtained from 3,4-bisbenzyloxyphenyl boronic acid and 5-bromo-N-cyclopropylthiophene-2-carboxamide [27] according to the procedure described for **14a** in 60%. TLC (SiO_2, 25% EtOAc/Hexane): R_f = 0.12. ^{1}H NMR ($CDCl_3$, 200 MHz) δ 0.69 (m, 2H), 0.79 (m, 2H), 2.63 (m, 1H), 4.88 (s, 2H), 4.99 (s, 2H), 5.82 (s, 1H), 6.72 (m, 1H), 6.82 (m, 2H), 6.69 (m, 2H), 7.10–7.30 (10H). MS (ESI(+)) *m/z* 456 $[M+H]^+$.

N-cyclopropyl-5-(3,4-dihydroxyphenyl)thiophene-2-carboxamide (16): was obtained from **16a** according to procedure for **14** in 40 %. TLC (SiO_2, 50% EtOAc/Hexane): R_f = 0.19. ^{1}H NMR (CD_3OD, 500 MHz) δ 0.64 (m, 2H), 0.79 (m, 2H), 2.80 (m, 1H), 6.79 (d, *J* = 8.5 Hz, 1H), 7.01 (dd, *J* = 8.0 Hz, 2.0 Hz, 1H), 7.08 (d, *J* = 2.0 Hz, 1H), 7.15 (d, *J* = 4.0 Hz, 1H), 7.55 (d, *J* = 4.0 Hz, 1H); ^{13}C NMR (CD_3OD, 125 MHz) δ 6.72, 24.01, 114.32, 117.00, 119.15, 123.31, 127.16, 130.84, 137.23, 146.99, 147.62, 151.53, 166.24. MS (ESI(+)) *m/z* 276 $[M+H]^+$; HRMS (ESI(−)) *m/z* 274.0545 (calcd for $C_{14}H_{12}NO_3S$ 274.0538).

2-(3,4-dimethoxyphenyl)thiophene (17a): was obtained from commercial available compound 3,4-dimethoxyphenylboronic acid and 2-bromothiophene according to the procedure described for **14a** in 50%. TLC (SiO_2, 5% EtOAc/Hexane): R_f = 0.20. ^{1}H NMR ($CDCl_3$, 200 MHz) δ 3.91 (s, 3H), 3.94 (s, 3H), 6.88 (d, *J* = 8.4 Hz, 1H), 7.06 (dd, *J* =5.0 Hz, 3.6 Hz, 1H), 7.11 (d, *J* = 1.8 Hz, 1H), 7.18 (dd, *J* = 8.4 Hz, 1.8 Hz, 1H), 7.20 (dd, *J* =3.6 Hz, 1.0 Hz, 1H), 7.23 (dd, *J* = 5.0 Hz, 1.0 Hz, 1H). MS (ESI(+)) *m/z* 221 $[M+H]^+$.

4-(thiophen-2-yl)benzene-1,2-diol (17): was obtained from **17a** in presence of BBr_3 according to the procedure described for **14** in 57%. TLC (SiO_2, 25% EtOAc/Hexane): R_f = 0.30. ^{1}H NMR (CD_3OD, 500 MHz) δ 6.76 (d, *J* = 8.5 Hz, 1H), 6.95 (dd, *J* = 8.0 Hz, 2.5 Hz, 1H), 7.00 (dd, *J* = 5.0 Hz, 3.5 Hz, 1H), 7.04 (d, *J* = 2.0 Hz, 1H), 7.15 (dd, *J* = 3.5 Hz, 1.0 Hz, 1H), 7.22 (dd, *J* = 5.5 Hz, 1.0 Hz, 1H); ^{13}C NMR (CD_3OD, 125 MHz) δ 114.24, 116.86, 118.79, 122.77, 124.39, 128.23, 128.89, 146.18, 146.44, 146.75. MS (ESI(+)) *m/z* 193 $[M+H]^+$; HRMS (EI) *m/z* 192.0236 (calcd for $C_{10}H_8O_2S$ 192.0245). HPLC purity: system A, t_R 6.29 min (99.12 %); system B, t_R 9.90 min (99.61 %).

2-(3,4-dimethoxyphenyl)-5-methylthiophene (18a): was obtained from commercial available compound 3,4-dimethoxyphenylboronic acid and 2-iodo-5-methylthiophene according to the procedure described for **14a** in 64%. TLC (SiO_2, 5% EtOAc/Hexane): R_f = 0.21. ^{1}H NMR ($CDCl_3$, 500 MHz) δ 2.49 (s, 3H), 3.89 (s, 3H), 3.92 (s, 3H), 6.70 (d, *J* = 3.5 Hz, 1H), 6.85 (d, *J* = 8.5 Hz, 1H), 6.99 (d, *J* = 3.5 Hz, 1H), 7.05 (d, *J* = 2.0 Hz, 1H), 7.10 (dd, *J* = 8.5 Hz, 2.0 Hz, 1H). MS (ESI(+)) *m/z* 235 $[M+H]^+$.

4-(5-methylthiophen-2-yl)benzene-1,2-diol (18): was obtained from **18a** in presence of BBr_3 according to the procedure described for **14** in 68%. TLC (SiO_2, 25% EtOAc/Hexane): R_f = 0.31. ^{1}H NMR (CD_3OD, 500 MHz) δ 2.43 (s, 3H), 6.64 (dd, *J* = 3.0 Hz, 1.0 Hz, 1H), 6.75 (d, *J* = 8.0 Hz, 1 H), 6.88 (dd, *J* = 2.0 Hz, 8.0 Hz, 1H), 6.91 (d, *J* = 3.5 Hz, 1H), 6.99 (d, *J* = 2.0 Hz, 1H); ^{13}C NMR (CD_3OD, 125 MHz) δ 15.31, 113.85, 116.81, 118.36, 122.51, 127.11, 128.59, 138.98, 143.83, 146.05, 146.65. MS (ESI(+)) *m/z* 207 $[M+H]^+$; HRMS (CI) *m/z* 206.0400 (calcd for $C_{11}H_{10}O_2S$ 206.0402). HPLC purity: system A, t_R 7.57 min (95.67 %); system B, t_R 10.93 min (97.44 %).

5-(3,4-dimethoxyphenyl)thiophene-2-carbonitrile (19a): was obtained from commercial available compound 3,4-dimethoxyphenylboronic acid and 5-bromothiophene-2-carbonitrile according to the procedure described for **14a** in 67%. TLC (SiO_2, 10% EtOAc/Hexane): R_f = 0.20. ^{1}H NMR ($CDCl_3$, 200 MHz) δ 3.93 (s, 3H), 3.95 (s, 3H), 6.91 (d, *J* = 8.4 Hz, 1H), 7.06 (d, *J* = 1.8 Hz, 1H), 7.17 (d, *J* = 4.4 Hz, 1H), 7.19 (m, 1H), 7.57 (d, *J* = 4.4 Hz, 1H). MS (ESI (+)) *m/z* 246 $[M+H]^+$.

5-(3,4-dihydroxyphenyl)thiophene-2-carbonitrile (19): was obtained from **19a** in presence of BBr_3 according to the procedure described for **14** in 68%. TLC (SiO_2, 25% EtOAc/Hexane): R_f = 0.14. ^{1}H NMR (CD_3OD, 500 MHz) δ 6.81 (d, *J* = 8.0 Hz, 1H), 7.04 (dd, *J* = 8.0 Hz, 2.5 Hz, 1H), 7.09 (d, *J* = 2.5 Hz, 1H), 7.26 (d, *J* = 4.0 Hz, 1H), 7.66 (d, *J* = 4.0 Hz, 1H); ^{13}C NMR (CD_3OD, 125 MHz) δ 107.11, 114.47, 115.54, 117.10, 119.60, 123.38, 125.67, 140.31, 147.21, 148.52, 154.34. MS (ESI(+)) *m/z* 218 $[M+H]^+$; HRMS (CI) *m/z* 217.0197 (calcd for $C_{11}H_7NO_2S$ 217.0197). HPLC purity: system A, t_R 6.25 min (99.30%); system B, t_R 7.02 min (99.68%).

2-chloro-5-(3,4-dimethoxyphenyl)thiophene (20a): was obtained from commercial available compound 3,4-dimethoxyphenylboronic acid and 2-bromo-5-chlorothiophene according to the procedure described for **14a** in 70%. TLC (SiO_2, 5% EtOAc/Hexane): R_f = 0.22. ^{1}H NMR ($CDCl_3$, 200 MHz) δ 3.90 (s, 3H), 3.92 (s, 3H), 6.857 (d, *J* = 4.0 Hz, 1H), 6.860 (d, *J* = 8.4 Hz, 1H), 6.95 (d, *J* = 3.6 Hz, 1H), 6.99 (d, *J* = 1.8 Hz, 1H), 7.06 (dd, *J* = 8.0 Hz, 2.0 Hz, 1H). MS (ESI(+)) *m/z* 255 $[M+H]^+$.

4-(5-chlorothiophen-2-yl)benzene-1,2-diol (20): was obtained from **20a** in presence of BBr_3 according to the procedure described for **14** in 45%. TLC (SiO_2, 25% EtOAc/Hexane): R_f = 0.35. ^{1}H NMR (CD_3OD, 500 MHz) δ 6.77 (d, *J* = 8.5 Hz, 1H), 6.86 (d, *J* = 4.0 Hz, 1H), 6.88 (dd, *J* = 8.5 Hz, 2.5 Hz, 1H), 6.95 (d, *J* = 4.0 Hz, 1H), 6.97 (d, *J* = 2.0 Hz, 1H); ^{13}C NMR (CD_3OD, 125 MHz) δ 113.78, 116.93, 118.50, 122.07, 127.17, 128.36, 132.11, 145.18, 146.91,

146.95. MS (ESI(−)) *m/z* 225 $[M-H]^-$; HRMS (CI) *m/z* 225.9852 (calcd for $C_{10}H_7ClO_2S$ 225.9855). HPLC purity: system A, t_R 8.42 min (96.68%); system B, t_R 11.90 min (99.60%).

2-(3,4-dimethoxyphenyl)-3-methylthiophene (21a): was obtained from commercial available compound 3,4-dimethoxyphenylboronic acid and 2-bromo-3-methylthiophene according to the procedure described for **14a** in 75%. TLC (SiO_2, 5% EtOAc/Hexane): R_f = 0.20. ^{1}H NMR ($CDCl_3$, 200 MHz) δ 2.31 (s, 3H), 3.91 (s, 3H), 3.92 (s, 3H), 6.91 (d, *J* = 8.0 Hz, 1H), 6.92 (d, *J* = 5.8 Hz, 1H), 6.97 (d, *J* = 1.8 Hz, 1H), 7.02 (d, *J* = 8.0 Hz, 2.2 Hz, 1H), 7.17 (d, *J* = 5.2 Hz, 1H). MS (ESI(+)) *m/z* 235 $[M+H]^+$.

4-(3-methylthiophen-2-yl)benzene-1,2-diol (21): was obtained from **21a** in presence of BBr_3 according to the procedure described for **14** in 50%. TLC (SiO_2, 25% EtOAc/Hexane): R_f = 0.33. ^{1}H NMR (CD_3OD, 500 MHz) δ 2.26 (s, 3H), 6.76 (dd, *J* = 8.0 Hz, 2.0 Hz, 1H), 6.80 (d, *J* = 8.5 Hz, 1H), 6.86 (d, *J* = 5.5 Hz, 1H), 6.87 (d, *J* = 2.0 Hz, 1H), 7.15 (d, *J* = 5.0Hz, 1H); ^{13}C NMR (CD_3OD, 125 MHz) δ 15.06, 116.53, 117.36, 121.91, 123.35, 128.12, 131.90, 133.28, 139.46, 146.10, 146.39. HRMS(CI) *m/z* 206.0399 (calcd for $C_{11}H_{10}O_2S$ 206.0402). HPLC purity: system A, t_R 7.23 min (99.83%); system B, t_R 10.59 min (99.01%).

2-(3,4-dimethoxyphenyl)-3-ethylthiophene (22a): was obtained from 3,4-dimethoxyphenylboronic acid and 2-bromo-3-ethylthiophene [28] according to the procedure described for **14a** in 81%. TLC (SiO_2, 5% EtOAc/Hexane): R_f = 0.21. ^{1}H NMR ($CDCl_3$, 200 MHz) δ 1.23 (t, *J* = 7.8 Hz, 3H), 2.68 (q, *J* = 7.6 Hz, 2H), 3.91 (s, 3H), 3.92 (s, 3H), 6.88–7.02 (4H), 7.20 (d, *J* = 5.0 Hz, 1H). MS (ESI(+)) *m/z* 249 $[M+H]^+$.

4-(3-ethylthiophen-2-yl)benzene-1,2-diol (22): was obtained from **22a** in presence of BBr_3 according to the procedure described for **14** in 71%. TLC (SiO_2, 25% EtOAc/Hexane): R_f = 0.33. ^{1}H NMR (CD_3OD, 500 MHz) δ 1.18 (t, *J* = 7.5 Hz, 3H), 2.64 (q, *J* = 7.5 Hz, 2H), 6.73 (dd, *J* = 8.0 Hz, 2.5 Hz, 1H), 6.81 (d, *J* = 8.0 Hz, 1H), 6.86 (d, *J* = 2.5 Hz, 1H), 6.93 (d, *J* = 5.0 Hz, 1H), 7.16 (d, *J* = 5.0 Hz, 1H); ^{13}C NMR (CD_3OD, 125 MHz) δ 16.01, 22.95, 116.50, 117.61, 122.16, 123.82, 127.99, 130.00, 139.09, 140.29, 146.15, 146.31. MS (ESI(−)) *m/z* 219 $[M-H]^-$; HRMS(CI) *m/z* 220.0555 (calcd for $C_{12}H_{12}O_2S$ 220.0558). HPLC purity: system A, t_R 8.71 min (99.72%); system B, t_R 11.30 min (99.39%).

2-(3,4-dimethoxyphenyl)-3-propylthiopene (23a): was obtained from 3,4-dimethoxyphenylboronic acid and 2-bromo-3-propylthiophene [28] according to the procedure described for **14a** in 70%. TLC (SiO_2, 5% EtOAc/Hexane): R_f = 0.22. ^{1}H NMR ($CDCl_3$, 200 MHz) δ 0.92 (t, *J* = 7.2 Hz, 3H), 1.65 (m, 2H), 2.62 (t, *J* = 7.8 Hz, 2H), 3.90 (s, 3H), 3.92 (s, 3H), 6.82–7.01 (4H), 7.19 (d, *J* = 5.4 Hz, 1H). MS (ESI(+)) *m/z* 263 $[M+H]^+$.

4-(3-propylthiophen-2-yl)benzene-1,2-diol (23): was obtained from **23a** in presence of BBr_3 according to the procedure described for **14** in 13%. TLC (SiO_2, 25% EtOAc/Hexane): R_f = 0.33. ^{1}H NMR (CD_3OD, 500 MHz) δ 0.89 (t, *J* = 7.5 Hz, 3H), 1.59 (m, 2H), 2.60 (t, *J* = 7.5 Hz, 2H), 6.72 (d, *J* = 8.0 Hz, 1H), 6.80 (d, *J* = 8.0 Hz, 1H), 6.85 (s, 1H), 6.91 (d, *J* = 5.0 Hz, 1H), 7.17 (d, *J* = 4.5 Hz, 1H); ^{13}C NMR (CD_3OD, 125 MHz) δ 14.39, 25.32, 31.81, 116.47, 117.77, 122.29, 123.69, 128.07, 130.38, 138.77, 139.64, 146.19, 146.33. MS (ESI(+)) *m/z* 235 $[M+H]^+$; HRMS(CI) *m/z* 234.0705 (calcd for $C_{13}H_{14}O_2S$ 234.0715). HPLC purity: system A, t_R 9.19 min (99.77%); system B, t_R 11.94 min (99.60%).

3-butyl-2-(3,4-dimethoxyphenyl)thiophene (24a): was obtained from 3,4-dimethoxyphenylboronic acid and 2-bromo-3-butylthiophene [28] according to the procedure described for **14a** in 72%. TLC (SiO_2, 5% EtOAc/Hexane): R_f = 0.19. ^{1}H NMR ($CDCl_3$, 200 MHz) δ 0.68 (t, *J* = 7.4 Hz, 3H), 1.13 (m, 2H), 1.39 (m, 2H), 2.45 (t, *J* = 7.4 Hz, 2H), 3.70 (s, 3H), 3.71 (s, 3H), 6.68–6.77 (4H), 6.98 (d, *J* = 5.4 Hz, 1H). MS (ESI(+)) *m/z* 277 $[M+H]^+$.

4-(3-butylthiophen-2-yl)benzene-1,2-diol (24): was obtained from **24a** in presence of BBr_3 according to the procedure described for **14** in 15%. TLC (SiO_2, 25% EtOAc/Hexane): R_f = 0.33. ^{1}H NMR (CD_3OD, 500 MHz) δ 0.87 (t, *J* = 7.5 Hz, 3H), 1.30 (m, 2H), 1.55 (m, 2H), 2.62 (t, *J* = 7.0 Hz, 2H), 6.71 (d, *J* = 8.0 Hz, 1 H), 6.79 (d, *J* = 8.0 Hz, 1H), 6.83 (d, *J* = 2.0 Hz, 1H), 6.91 (d, *J* = 5.0 Hz, 1H), 7.61 (d, *J* = 3.5 Hz, 1H); ^{13}C NMR (CD_3OD, 125 MHz) δ 14.31, 23.60, 29.38, 34.45, 116.47, 117.78, 122.29, 123.72, 128.06, 130.37, 138.93, 139.53, 146.20, 146.35. MS (ESI(+)) *m/z* 249 $[M+H]^+$; HRMS(CI) *m/z* 248.0858 (calcd for $C_{14}H_{16}O_2S$ 248.0871). HPLC purity: system A, t_R 10.25 min (99.96%); system B, t_R 12.57 min (99.01%).

2-(2-(3,4-dimethoxyphenyl)thiophen-3-yl)ethanol (25a): was obtained from 3,4-dimethoxyphenylboronic acid and 2-(2-bromothiophen-3-yl)ethanol [28] according to the procedure described for **14a** in 50%. TLC (SiO_2, 30% EtOAc/Hexane): R_f = 0.15. ^{1}H NMR ($CDCl_3$, 200 MHz) δ 2.95 (t, *J* = 6.2 Hz, 3H), 3.84 (t, *J* = 6.6 Hz, 2H), 3.91 (s, 3H), 3.92 (s, 3H), 6.93 (m, 1H), 7.00(m, 2H), 7.25 (m, 2H).

4-(3-(2-bromoethyl)thiophen-2-yl)benzene-1,2-diol (25): was obtained from **25a** in presence of BBr_3 according to the procedure described for **14** in 38%. TLC (SiO_2, 25% EtOAc/Hexane): R_f = 0.30. ^{1}H NMR (CD_3OD, 500 MHz) δ 3.17 (t, *J* = 7.5 Hz, 2H), 3.53 (t, *J* = 7.5 Hz, 2H), 6.74 (dd, *J* = 8.5 Hz, 2.0 Hz, 1H), 6.81 (d, *J* = 8.5 Hz, 1H), 6.84 (d, *J* = 2.0 Hz, 1H), 6.99 (d, *J* = 5.0 Hz, 1H), 7.23 (d, *J* = 5.0 Hz, 1H); ^{13}C NMR (CD_3OD, 125 MHz) δ 32.78, 33.50, 116.65, 117.71, 122.27, 124.32, 127.23, 130.00, 135.43, 141.62, 146.56, 146.64. MS (ESI(+)) *m/z* 299/301 $[M+H]^+$; HRMS(CI) *m/z* 297.9653 (calcd for $C_{12}H_{11}BrO_2S$ 297.9663). HPLC purity: system A, t_R 8.54 min (99.33%); system B, t_R 11.42 min (98.10%).

3-(3,4-dimethoxyphenyl)thiophene (26a): was obtained from commercial available compound 3,4-dimethoxyphenylboronic acid and 3-bromothiophene according to the procedure described for **14a** in 64%. TLC (SiO_2, 5% EtOAc/Hexane): R_f = 0.20. ^{1}H NMR ($CDCl_3$, 200 MHz) δ 3.91 (s, 3H), 3.94 (s, 3H), 6.90 (d, *J* = 8.4 Hz, 1H), 7.10 (d, *J* = 1.8 Hz, 1H), 7.15 (dd, *J* = 8.4 Hz, 1.8 Hz, 1H), 7.32–7.38 (3H). MS (ESI(+)) *m/z* 221 $[M+H]^+$.

4-(thiophen-3-yl)benzene-1,2-diol (26): was obtained from **26a** in presence of BBr_3 according to the procedure described for **14** in 57%. TLC (SiO_2, 25% EtOAc/Hexane): R_f = 0.32. ^{1}H NMR (CD_3OD, 500 MHz) δ 6.77 (d, *J* = 8.0 Hz, 1H), 6.97 (dd, *J* = 8.0 Hz, 2.5 Hz, 1H), 7.06 (d, *J* = 2.5 Hz, 1H), 7.32 (dd, *J* = 5.0 Hz, 1.0 Hz, 1H), 7.37 (dd, *J* = 3.0 Hz, 1 Hz, 1H), 7.39 (dd, *J* = 5.0 Hz, 3.0 Hz, 1H); ^{13}C NMR (CD_3OD, 125 MHz) δ 114.68, 116.79, 119.16, 119.37, 126.86, 127.17, 129.74, 143.87, 145.90, 146.62. MS (ESI(+)) *m/z* 193 $[M+H]^+$; HRMS (EI) *m/z* 192.0238 (calcd for $C_{10}H_8O_2S$ 192.0245). HPLC purity: system A, t_R 6.07 min (97.24%); system B, t_R 9.59 min (98.16%).

3-(3,4-dimethoxyphenyl)-2,5-dimethylthiophene (27a): was obtained from 3,4-dimethylphenylboronic acid and 3-iodo-2,5-dimethylthiophene-2,5-dimethylthiophene [29] according to the procedure described for **14a** in 90%. TLC (SiO_2, 5% EtOAc/Hexane): R_f = 0.28. ^{1}H NMR ($CDCl_3$, 200 MHz) δ 2.43 (s, 3H), 2.44 (s, 3H), 3.90 (s, 3H), 3.91 (s, 3H), 6.68 (1H), 6.89–6.91 (3H). MS (ESI(+)) *m/z* 249 $[M+H]^+$.

4-(2,5-dimethylthiophen-3-yl)benzene-1,2-diol (27): was obtained from **27a** in presence of BBr_3 according to the procedure described for **14** in 90%. TLC (SiO_2, 25% EtOAc/Hexane): R_f = 0.34. ^{1}H NMR (CD_3OD, 500 MHz) δ 2.36 (s, 3H), 2.37 (s, 3H), 6.59 (s, 1H), 6.66 (m, 1H), 6.78 (m, 2H); ^{13}C NMR (CD_3OD, 125 MHz) δ 14.31, 15.15, 116.38, 116.88, 121.37, 127.55, 128.49, 130.53, 136.15, 139.75, 145.26, 146.14. MS (ESI(+)) *m/z* 221 $[M+H]^+$; HRMS (CI) *m/z* 220.0551 (calcd for $C_{12}H_{12}O_2S$ 220.0558). HPLC purity: system A, t_R 9.61 min (98.52%); system B, t_R 12.31 min (99.55%).

3-(3,4-bis(benzyloxy)phenyl)-2,5-dichlorothiophene (28a): was obtained from 3,4-bis (benzyloxy)phenylboronic acid and 3-bromo-2,5-dichlorothiophene according to the procedure described for **14a** in 68%. TLC (SiO_2, 5% EtOAc/Hexane): R_f = 0.51. ^{1}H NMR ($CDCl_3$, 500 MHz) δ 5.198 (s, 2H), 5.202 (s, 2H), 6.81 (s, 1H), 6.97 (d, *J* = 8.0 Hz, 1H), 7.01 (dd, *J* = 8.0 Hz, 2.0 Hz, 1H), 7.12 (d, *J* = 2.0 Hz, 1H), 7.32 (m, 2H), 7.37 (m, 4H), 7.45 (m, 4H). MS (ESI(+)) *m/z* 463 $[M+Na]^+$.

4-(2,5-dichlorothiophen-3-yl)benzene-1,2-diol (28): was obtained from **28a** in presence of BCl_3 according to the procedure described for **14** in 57%. TLC (SiO_2, 25% EtOAc/Hexane): R_f = 0.37. ^{1}H NMR (CD_3OD, 500 MHz) δ 6.81 (d, *J* = 8.0 Hz, 1H), 6.86 (dd, *J* = 8.0 Hz, 2.0 Hz, 1H), 6.97 (s, 1H), 6.99 (d, *J* = 2.0 Hz, 1H); ^{13}C NMR (CD^3OD, 125 MHz) δ 116.54, 116.69, 121.15, 121.48, 126.38, 127.03, 129.19, 140.10, 146.43, 146.84. MS (ESI(+)) *m/z* 259/261 $[M-H]^-$; HRMS(CI) *m/z* 259.9459 (calcd for $C_{10}H_6C_{l2}O_2S$ 259.9466). HPLC purity: system A, t_R 9.75 min (99.80%); system B, t_R 12.72 min (99.00%).

3-bromo-4-(3,4-dimethoxyphenyl)-2,5-dimethylthiophene (29a): was obtained from 3,4-dimethylphenylboronic acid and 3,4-dibromo-2,5-dimethylthiophene [30] according to the procedure described for **14a** in 31%. TLC (SiO_2, 5% EtOAc/Hexane): R_f = 0.30. ^{1}H NMR ($CDCl_3$, 200 MHz) δ 2.31 (s, 3H), 2.40 (s, 3H), 3.89 (s, 3H), 3.92 (s, 3H), 6.82 (m, 2H), 6.93 (d, *J* = 8.8 Hz, 1H). MS (ESI(+)) *m/z* 327/329 $[M+H]^+$.

4-(4-bromo-2,5-dimethylthiophen-3-yl)benzene-1,2-diol (29): was obtained from **29a** in presence of BBr_3 according to the procedure described for **14** in 40%. TLC (SiO_2, 25% EtOAc/Hexane): R_f = 0.40. ^{1}H NMR (CD^3OD, 500 MHz) δ 2.26 (s, 3H), 2.34 (s, 3H), 6.53 (d, *J* = 8.0 Hz, 1H), 6.66 (s, 1H), 6.80 (d, *J* = 8.0 Hz, 1H); ^{13}C NMR (CD_3OD, 125 MHz) δ 14.58, 15.18, 112.26, 116.15, 118.57, 123.08,128.48, 129.07, 130.92, 132.87, 139.97, 146.00. MS (ESI(+)) m/z 299/301 $[M+H]^+$; HRMS(CI) *m/z* 297.9655 (calcd for $C_{12}H_{11}BrO_2S$ 297.9663). HPLC purity: system A, t_R 9.56 min (99.30%); system B,t_R 12.29 min (99.42%).

MetAP enzymatic activity assay: The recombinant *E. coli* MetAP was purified from BL21 (DE3) cells as apoenzyme [9]. Met-AMC was purchased from Bachem Bioscience (King of Prussia, PA).Enzyme activity was monitored by following the hydrolysis of MetAMC (λex 360 nm, λem 460) on a SpectraMax Gemini XPS plate reader (Molecular Devices, Sunnyvale, CA), carried out on 384-well plates at room temperature. The assay consisted of an 80 μL assay mixture containing 50 mM MOPS (pH 7.0), 200 μM Met-AMC, 500 nM apoenzyme, metal ions (50 μM $FeCl_2$ with 100 μM ascorbic acid, 10 μM $CoCl_2$, or 20 μM $MnCl_2$) and an inhibitor at serially diluted concentrations. The IC_{50} values were calculated from non-linear curve fitting procedures of percent inhibition as a function of inhibitor concentrations.

High throughput screening: A chemical library of 74,976 small organic molecules used for screening was purchased from ChemBridge and ChemDiv (both at San Diego, CA), and these compounds were selected from vendors' much larger compound collections for structural diversity and drug-like properties. Reactive, unstable and potentially toxic compounds were eliminated in the selection process. All compounds have molecular weight between 150 and 480 and calculated LogP (cLogP) below 5. The assay was performed on 384-well flat-bottom polystyrene microplates on a SpectraMax Gemini XS microplate fluorescence reader (Molecular Devices Corp., Sunnyvale, CA). The screening compounds were distributed on 213 plates at a final compound concentration of 6.25 μg/mL. Each plate had 352 compound wells and 32 positive and negative control wells. The negative control wells contained no screening compounds, and the positive control wells contained no screening compounds and no apoenzyme. The assay mixture (80 μL final volume) contains 50 mM MOPS (pH 7.0), 1.0 μM apo-MetAP, 200 μM Met-AMC, and 4 μM $FeCl_2$. Screening hits were ranked according to their potencies (percent inhibition), and the top ranked 320 hits with a cut-off at 84% inhibition

were selected for confirmation of inhibitory activity by determining their IC_{50} values using 6 serially diluted concentrations. Liquid handling for hit-picking and serial dilutions was carried out on a Biomek FX liquid handling workstation (Beckman Coulter Inc., Fullerton, CA) and a Precision 2000 automated microplate pipetting system (BioTek Instruments Inc, Winooski, VT).

Bacterial growth inhibition assay: *Bacillus megaterium*, *Bacillus subtilis*, and *E. coli* ATCC 25922 were acquired from Fisher (Pittsburgh, PA). *E. coli* strain D22 [25] was obtained from the *E. coli* Genetic Stock Center at Yale (http://cgsc.biology.yale.edu/). *E. coli* strain AS19 was obtained as a gift from Dr. Liam Good at Karolinska Institute. Strain AS19 has a severely depleted lipopolysaccharides (LPS) layer [24], but its exact mutation is unknown. Bacterial strains (*E. coli* AS19, *E. Coli* D22, *Bacillus megaterium* and *B. subtilis*) grown to exponential phase with 0.5 McFarland optical density [31] was diluted 1000 fold in Mueller Hinton media containing 100 mM Tris pH 7.5, which were then dispensed in 40 μL volumes into an opaque 384-well plate containing 20 μL of inhibitor at increasing concentrations, followed by addition of 20 μL of resazurin for a final concentration of 110 μM. Cell growth was monitored kinetically by fluorescence (λex 530 nm, λem 590) for 10 hours with 5 min intervals at 37°C. In the case of *E. coli* AS19, resazurin was omitted and the signal monitored by absorbance at 600 nm, because the absorbance signal was much more stable for *E. coli* AS19 than for the other strains tested. Fluorescence or absorbance values corresponding to 50–85% of total intensity of an uninhibited sample were averaged and converted to percent inhibition to obtain IC_{50} values as described above. MIC values were calculated as the concentration of compound resulting in 90% inhibition of cell growth. Assay was performed for *E. coli* ATCC 25922 in the presence of resazurin as described above, with the exception that Tris was not included in the culture medium.

Crystallization and data collection: Crystals of the enzyme-inhibitor complex were obtained by hanging-drop vapor-diffusion method at room temperature. Inhibitor **22** (100 mM in DMSO) was added to concentrated apoenzyme (10 mg/mL, 0.4 mM) in 50 mM Tris.HCl (pH 7.8), and the molar ratio of **22** to MetAP was 6:1. The enzyme/inhibitor mixture was mixed with the reservoir buffer (100 mM MES, pH 6.5, 2 mM $MnCl_2$, and 17% PEG 20,000) in a 1:1 ratio. Crystals were seen after about 3 days. After one crystal was picked up from the mother liquor with a fiber loop, the loop was dipped into a cryo solution containing 23% glycerol plus the reservoir solution and then immediately frozen in a nitrogen liquid stream. Diffraction data to 2.2 Å were collected over 180° in 0.5° increments using an in-house Cu Kα radiation source at 100 K. Raw reflection data were indexed and integrated using MOSFLM [32] and merged and scaled using SCALA in CCP4 [33] with CCP4i interface [34]. The crystal belongs to space group $P2_1$. One molecule is in the asymmetric unit.

Structural solution and refinement: The structure was solved by molecular replacement with the program Phaser [35]. The search model is the coordinates of an unligated *E. coli* methionine aminopeptidase (PDB code 2MAT) with metal ions and water molecules being removed. The structure was refined with REFMAC5 [36] with iterative model building using the program WinCoot [37]. The refinement was monitored using 5% of the reflections set aside for free R factor analysis throughout the whole refinement process. After MetAP protein, two Mn atoms and most of water molecules were modeled, an $F_{obs} - F_{calc}$ electron density difference map contoured at 2.5 σ level (Fig. 2) clearly showed the presence of the inhibitor **22**. The inhibitor was then added according to the density map. The final structure was analyzed using the program PROCHECK [38]. 99.6% of the main-chain angles of the residues are in the allowed region, and the residue in 0.4% disallowed regions is Asn-74, which remains the same conformation in other *E. coli* MetAP structures. The resulting map showed clear electron densities for most of the atoms except for a few side chain atoms on the molecular surface. Comparison of structures and generation of structural drawings were carried out by using

PyMOL [39]. Statistic parameters in data collection and structural refinement are shown in Table 2.

Abbreviations

MetAP, methionine aminopeptidase; AMC, 7-amino-4-methylcoumarin; rmsd, root mean square deviation; IC_{50}, concentration that causes 50% inhibition; MIC, minimum inhibitory concentration; PDB, protein data bank.

Acknowledgment

This research was supported by NIH grant AI065898 (Q.-Z. Y.). The High Throughput Screening Laboratory at University of Kansas was supported by NIH grant RR015563 from the COBRE program of the National Center for Research Resources, University of Kansas, and Kansas Technology Enterprise Corporation. We thank Dr. Liam Good for providing us *E. coli* AS19 strain for the testing.

References

1. Bradshaw RA, Brickey WW, Walker KW. N-terminal processing: the methionine aminopeptidase and N alpha-acetyl transferase families. Trends Biochem Sci 1998;23:263–267. [PubMed: 9697417]
2. Vaughan MD, Sampson PB, Honek JF. Methionine in and out of proteins: targets for drug design. Curr Med Chem 2002;9:385–409. [PubMed: 11860363]
3. Luo QL, Li JY, Liu ZY, Chen LL, Li J, Qian Z, Shen Q, Li Y, Lushington GH, Ye QZ, Nan FJ. Discovery and structural modification of inhibitors of methionine aminopeptidases from Escherichia coli and Saccharomyces cerevisiae. J Med Chem 2003;46:2631–2640. [PubMed: 12801227]
4. Schiffmann R, Heine A, Klebe G, Klein CD. Metal ions as cofactors for the binding of inhibitors to methionine aminopeptidase: A critical view of the relevance of in vitro metalloenzyme assays. Angew Chem Int Ed Engl 2005;44:3620–3623. [PubMed: 15880695]
5. Douangamath A, Dale GE, D'Arcy A, Almstetter M, Eckl R, Frutos-Hoener A, Henkel B, Illgen K, Nerdinger S, Schulz H, Mac Sweeney A, Thormann M, Treml A, Pierau S, Wadman S, Oefner C. Crystal structures of Staphylococcusaureus methionine aminopeptidase complexed with keto heterocycle and aminoketone inhibitors reveal the formation of a tetrahedral intermediate. J Med Chem 2004;47:1325–1328. [PubMed: 14998322]
6. Chang SY, McGary EC, Chang S. Methionine aminopeptidase gene of Escherichia coli is essential for cell growth. J Bacteriol 1989;171:4071–4072. [PubMed: 2544569]
7. Miller CG, Kukral AM, Miller JL, Movva NR. pepM is an essential gene in Salmonella typhimurium. J Bacteriol 1989;171:5215–5217. [PubMed: 2670909]
8. D'Souza VM, Holz RC. The methionyl aminopeptidase from Escherichia coli can function as an iron (II) enzyme. Biochemistry 1999;38:11079–11085. [PubMed: 10460163]
9. Li JY, Chen LL, Cui YM, Luo QL, Li J, Nan FJ, Ye QZ. Specificity for inhibitors of metal-substituted methionine aminopeptidase. Biochem Biophys Res Commun 2003;307:172–179. [PubMed: 12849997]
10. Lowther WT, Matthews BW. Structure and function of the methionine aminopeptidases. Biochim Biophys Acta 2000;1477:157–167. [PubMed: 10708856]
11. Ye QZ, Xie SX, Huang M, Huang WJ, Lu JP, Ma ZQ. Metalloform-selective inhibitors of escherichia coli methionine aminopeptidase and X-ray structure of a Mn(II)-form enzyme complexed with an inhibitor. J Am Chem Soc 2004;126:13940–13941. [PubMed: 15506752]
12. Walker KW, Bradshaw RA. Yeast methionine aminopeptidase I can utilize either Zn2+ or Co2+ as a cofactor: a case of mistaken identity? Protein Sci 1998;7:2684–2687. [PubMed: 9865965]
13. Yang G, Kirkpatrick RB, Ho T, Zhang GF, Liang PH, Johanson KO, Casper DJ, Doyle ML, Marino JP Jr, Thompson SK, Chen W, Tew DG, Meek TD. Steady-state kinetic characterization of substrates and metal-ion specificities of the full-length and N-terminally truncated recombinant human methionine aminopeptidases (type 2). Biochemistry 2001;40:10645–10654. [PubMed: 11524009]

14. D'Souza VM, Swierczek SI, Cosper NJ, Meng L, Ruebush S, Copik AJ, Scott RA, Holz RC. Kinetic and structural characterization of manganese(II)-loaded methionyl aminopeptidases. Biochemistry 2002;41:13096–13105. [PubMed: 12390038]
15. Wang J, Sheppard GS, Lou P, Kawai M, Park C, Egan DA, Schneider A, Bouska J, Lesniewski R, Henkin J. Physiologically relevant metal cofactor for methionine aminopeptidase-2 is manganese. Biochemistry 2003;42:5035–5042. [PubMed: 12718546]
16. Zhang JH, Chung TD, Oldenburg KR. A simple statistical parameter for use in evaluation and validation of high throughput screening assays. J Biomol Screen 1999;4:67–73. [PubMed: 10838414]
17. Mee SP, Lee V, Baldwin JE, Cowley A. Total synthesis of 5,5',6,6'-tetrahydroxy-3,3'-biindolyl, the proposed structure of a potent antioxidant found in beetroot (Beta vulgaris). Tetrahedron 2004;60:3695–3721.
18. Barton A, Breukelman SP, Kaye PT, Denis Meakins G, Morgan DJ. The preparation of thiazole-4- and -5-carboxylates, and an infrared study of their rotational isomers. J. Chem. Soc. Perkin. Trans. 1 1982:159–164.
19. Handy ST, Zhang Y, Bregman H. A modular synthesis of the lamellarins: total synthesis of lamellarin G trimethyl ether. J Org Chem 2004;69:2362–2366. [PubMed: 15049631]
20. Huang QQ, Huang M, Nan FJ, Ye QZ. Metalloform-selective inhibition: Synthesis and structure-activity analysis of Mn(II)-form-selective inhibitors of Escherichia coli methionine aminopeptidase. Bioorg Med Chem Lett 2005;15:5386–5391. [PubMed: 16219464]
21. Xie SX, Huang WJ, Ma ZQ, Huang M, Hanzlik RP, Ye QZ. Structural analysis of metalloform-selective inhibition of methionine aminopeptidase. Acta Crystallogr D Biol Crystallogr 2006;62:425–432. [PubMed: 16552144]
22. Jo DH, Chiou YM, Que L Jr. Models for extradiol cleaving catechol dioxygenases: syntheses, structures, and reactivities of iron(II)-monoanionic catecholate complexes. Inorg Chem 2001;40:3181–3190. [PubMed: 11399191]
23. Crosa JH, Walsh CT. Genetics and assembly line enzymology of siderophore biosynthesis in bacteria. Microbiol Mol Biol Rev 2002;66:223–249. [PubMed: 12040125]
24. Zorzopulos J, de Long S, Chapman V, Kozloff LM. Evidence for a net-like organization of lipopolysaccharide particles in the Escherichia coli outer membrane. FEMS Microbiol Lett 1989;52:23–26. [PubMed: 2689280]
25. Normark S, Boman HG, Matsson E. Mutant of Escherichia coli with anomalous cell division and ability to decrease episomally and chromosomally mediated resistance to ampicillin and several other antibiotics. J Bacteriol 1969;97:1334–1342. [PubMed: 4887513]
26. Cammidge AN, King ASH. Model studies towards liquid crystalline dendrimers with mesogenic repeat units throughout the structure. Tetrahedron Lett 2006;47:5569–5572.
27. Luo QL, Li JY, Chen LL, Li J, Ye QZ, Nan FJ. Inhibitors of type I MetAPs containing pyridine-2-carboxylic acid thiazol-2-ylamide. Part 2: SAR studies on the pyridine ring 3-substituent. Bioorg Med Chem Lett 2005;15:639–644. [PubMed: 15664829]
28. Herland A, Nilsson KP, Olsson JD, Hammarstrom P, Konradsson P, Inganas O. Synthesis of a regioregular zwitterionic conjugated oligoelectrolyte, usable as an optical probe for detection of amyloid fibril formation at acidic pH. J Am Chem Soc 2005;127:2317–2323. [PubMed: 15713111]
29. Pu S, Liu G, Li G, Yang T. Photochromic thiophene pyrrole mixed linkage type dithienylethene compounds, and their synthesizing and use. Faming Zhuanli Shenqing Gongkai Shuomingshu. 2007application number CN1978444
30. Cook MJ, Jafari-Fini A. Phthalocyanine-related macrocycles: cross cyclotetramerisation products from 3,4-dicyanothiophenes, 2,3-dicyanothiophene and 3,6-dialkylphthalonitriles. Tetrahedron 2000;56:4085–4094.
31. NCCLS. Methods for determining bactericidal activity of antimicrobial agents. Approved guideline. M26-A. Vol. Vol. 19. Payne, PA: National Committee for Clinical Laboratory Standards (Now Clinical and Laboratory Standards Institute); 1999.
32. Leslie AGW. Recent changes to the MOSFLM package for processing film and image plate data. Joint CCP4 + ESF-EAMCB Newsletter on Protein Crystallography No. 26. 1992
33. Collaborative Computational Project Number 4. The CCP4 Suite: Programs for Protein Crystallography. Acta Cryst 1994;D50:760–763.

34. Potterton E, Briggs P, Turkenburg M, Dodson E. A graphical user interface to the CCP4 program suite. Acta Crystallogr D Biol Crystallogr 2003;59:1131–1137. [PubMed: 12832755]

35. Read RJ. Pushing the boundaries of molecular replacement with maximum likelihood. Acta Crystallogr D Biol Crystallogr 2001;57:1373–1382. [PubMed: 11567148]

36. Murshudov GN, Vagin AA, Dodson EJ. Refinement of macromolecular structures by the maximum-likelihood method. Acta Crystallogr D Biol Crystallogr 1997;53:240–255. [PubMed: 15299926]

37. Emsley P, Cowtan K. Coot: model-building tools for molecular graphics. Acta Crystallogr D Biol Crystallogr 2004;60:2126–2132. [PubMed: 15572765]

38. Laskowski RA, MacArthur MW, Moss DS, Thornton JM. PROCHECK: a program to check the stereochemical quality of protein structures. J Appl Cryst 1993;26:283–291.

39. DeLano WL. The PyMOL Molecular Graphics System. 2002on World Wide Web http://www.pymol.org.

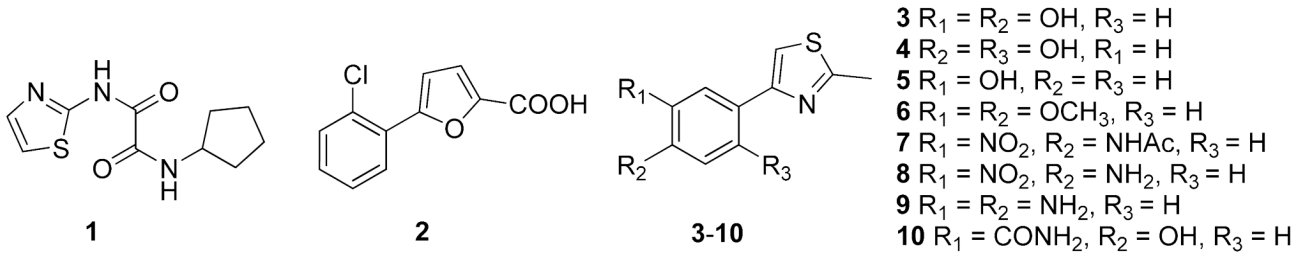

Figure 1.
Metalloform selective inhibitors of *E. coli* MetAP. Previously discovered **1** and **2** are selective for the Co(II)-form and the Mn(II)-form, respectively. The newly discovered **3** is selective for the Fe(II)-form. We synthesized **4–10** as derivatives of **3**.

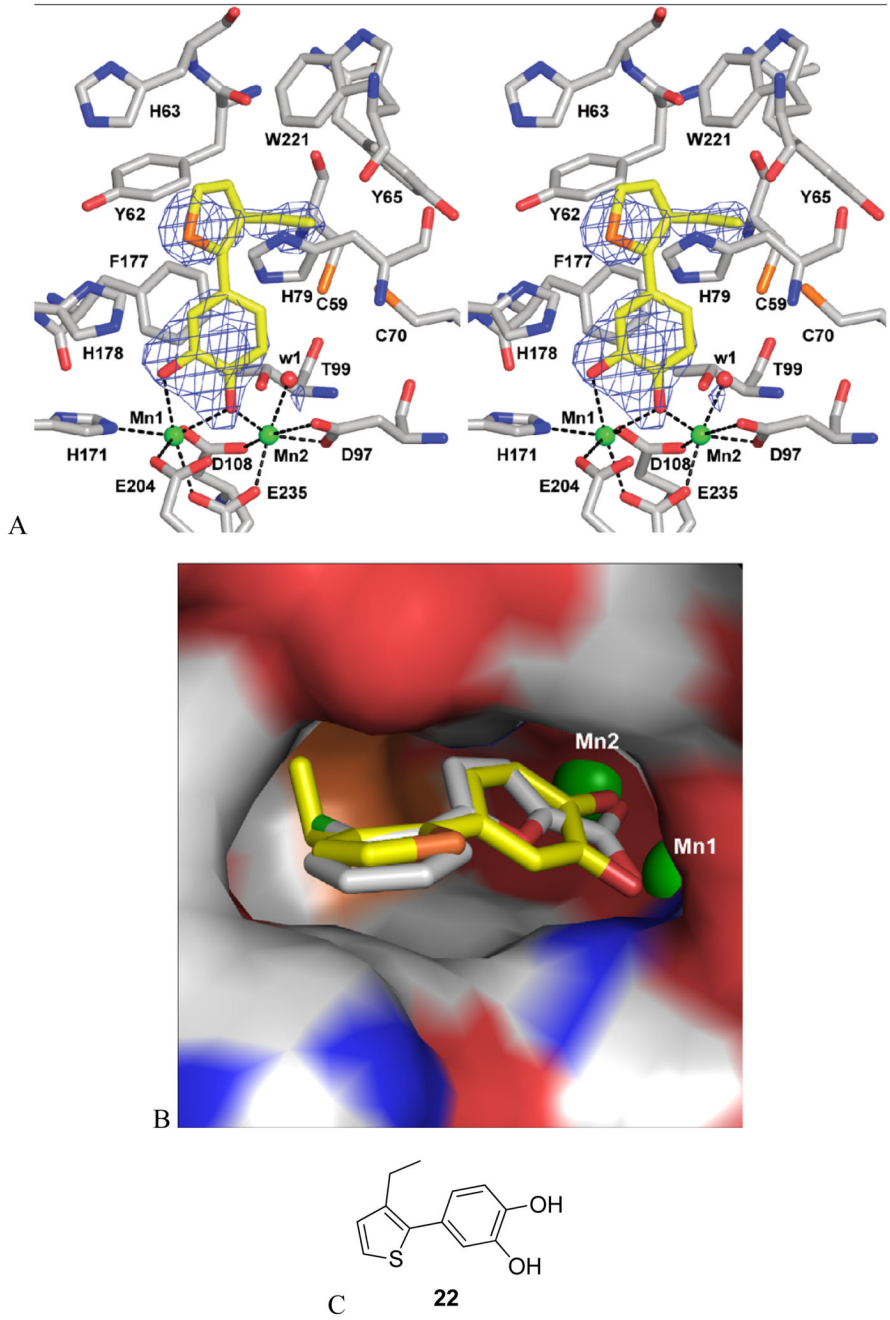

Figure 2.

X-ray structure of *E. coli* MetAP in complex with **22**. **A**. Stereo view of the ligand **22** at the binding pocket. The ligand and the residues at the binding site are shown as sticks (carbon yellow for **22** or grey for the protein residues, nitrogen blue, oxygen red, and sulfur orange), Mn(II) ions are shown as green spheres (Mn1 and Mn2), and a conserved water molecule is shown as a red sphere. $F_{obs} - F_{calc}$ difference map (before **22** was modeled in) is shown superimposed on the refined structure as blue meshes contoured at 2.5 σ. Interactions with the metal ions are shown as black dashed lines. **B**. Close-up view of **22**, in comparison with **2**, at the substrate binding pocket. The structure of the Fe(II)-form selective inhibitor **22** (carbon yellow) was superimposed with that of the Mn(II)-form selective inhibitor **2** (carbon grey).

The pocket is shown as surface with colors coded by atom types. Mn(II) ions are shown as partially buried green spheres. **C**. Chemical structure of **22**.

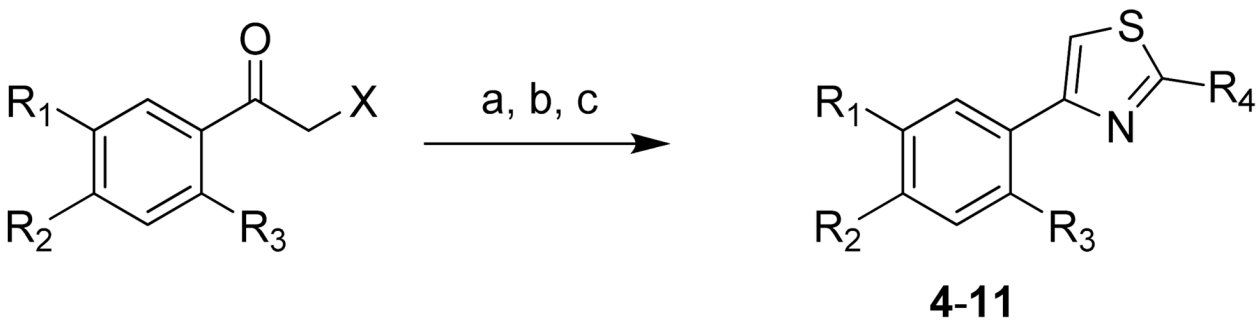

Scheme 1.

Syntheses of 4-phenylthiazolesa

[a] Reagents and conditions: (a) Ethanethioamide and X = Br for **4**, **5**, **6**, **10**; ethanethioamide and X = Cl for **7**; thiourea and X = Cl for **11**. MeOH, reflux, 80–90% yield. (b) For converting **7** to **8**, 6 N HCl, MeOH, reflux, 50%. (c) For converting **8** to **9**, H_2, 10% Pd/C, MeOH, overnight, 70%.

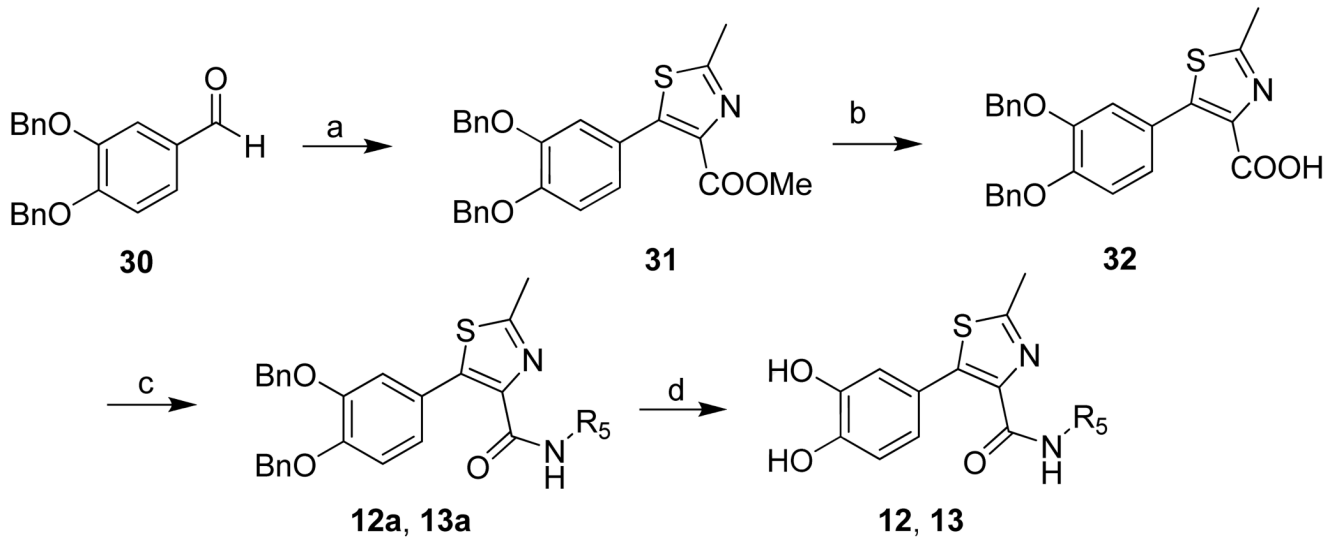

Scheme 2.

Syntheses of 5-phenylthiazolesa

[a] Reagents and conditions: (a) methyl dichloroacetate, Na, MeOH, 0°C; then ethanethioamide, THF, reflux, 43%. (b) LiOH, MeOH. (c) Amine, EDCI, DMAP, CH_2Cl_2, 63–70%. (d) BCl_3, CH_2Cl_2, −78°C, 36–50%.

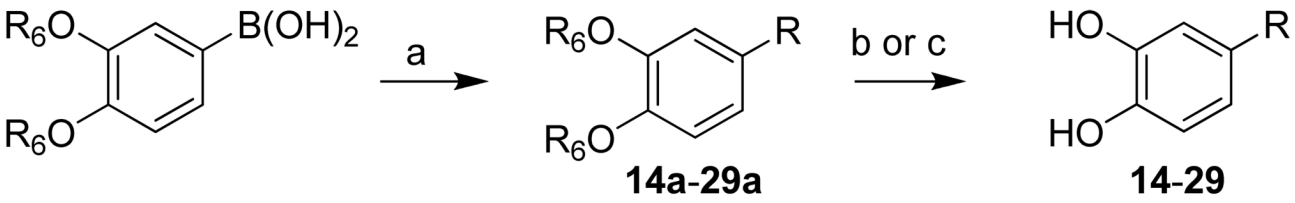

Scheme 3.

Syntheses of 2-phenylthiazoles and 2-thiophenes and 3-phenylthiophenes[a]

[a] Reagents and conditions: (a) $Pd(PPh_3)_4$, 2 N Na_2CO_3, RX (X = Br or I), DMF, 90 °C (R_6 = Bn for **14–16**; R^6 = Me for **17–29**), 31–90%. (b) For **14–16**, 1 M BCl_3, DCM, −78°C, 32–73%. (c) For **17–29**, 1 M BBr_3, DCM, −78°C, 13–90%.

Table 1

e activity and bacterial growth by the catechol-containing MetAP inhibitors [a, b]

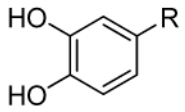

	Inhibition of enzymatic activity, IC_{50}, μM			Inhibition of bacterial growth, IC_{50}, μM [c]			
	Co(II)	**Mn(II)**	**Fe(II)**	***E. coli* AS19**	***E. coli* D22**	***B. subtilis***	***B. megaterium***
	>100	>100	13.0	117 (91)	5.6 (4)	67.0 (41)	69.8 (73)
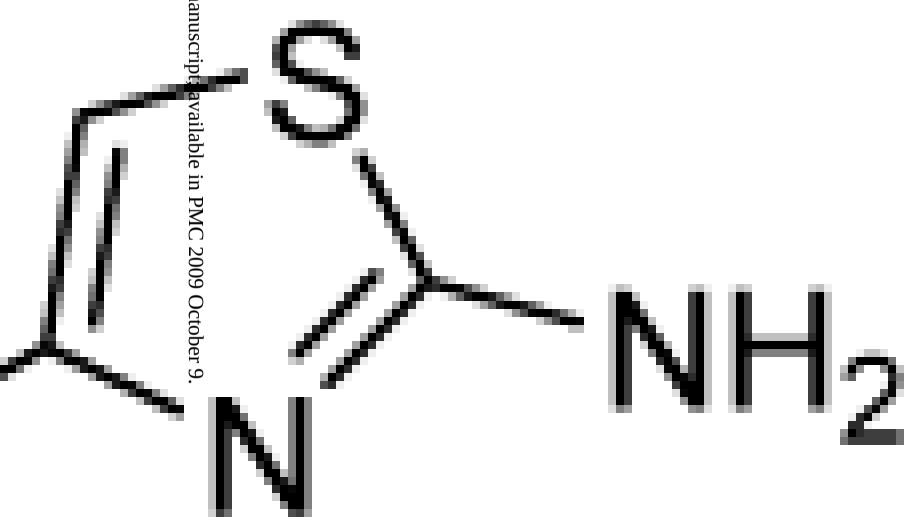	>100	>100	6.6	145 (39)	39.9 (11)	28.6 (13)	36.9 (26)

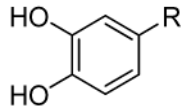

	Inhibition of enzymatic activity, IC_{50}, μM			Inhibition of bacterial growth, IC_{50}, μM [c]			
Co(II)	**Mn(II)**	**Fe(II)**	***E. coli* AS19**	***E. coli* D22**	***B. subtilis***	***B. megaterium***
92.3	100	11.1	125 (138)	166.8 (103)	113 (51)	75.5 (62)

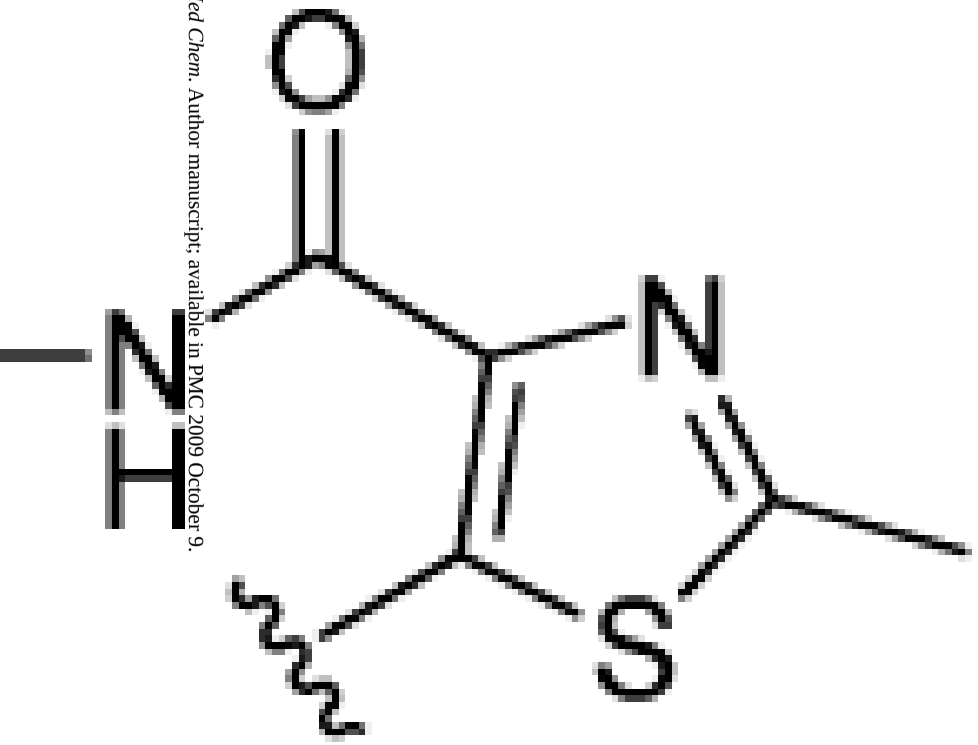

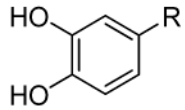

	Inhibition of enzymatic activity, IC_{50}, μM			Inhibition of bacterial growth, IC_{50}, μM [c]			
Co(II)	**Mn(II)**	**Fe(II)**	***E. coli* AS19**	***E. coli* D22**	***B. subtilis***	***B. megaterium***
>100	>100	15.4	116 (121)	93.8 (73)	186 (125)	175 (122)

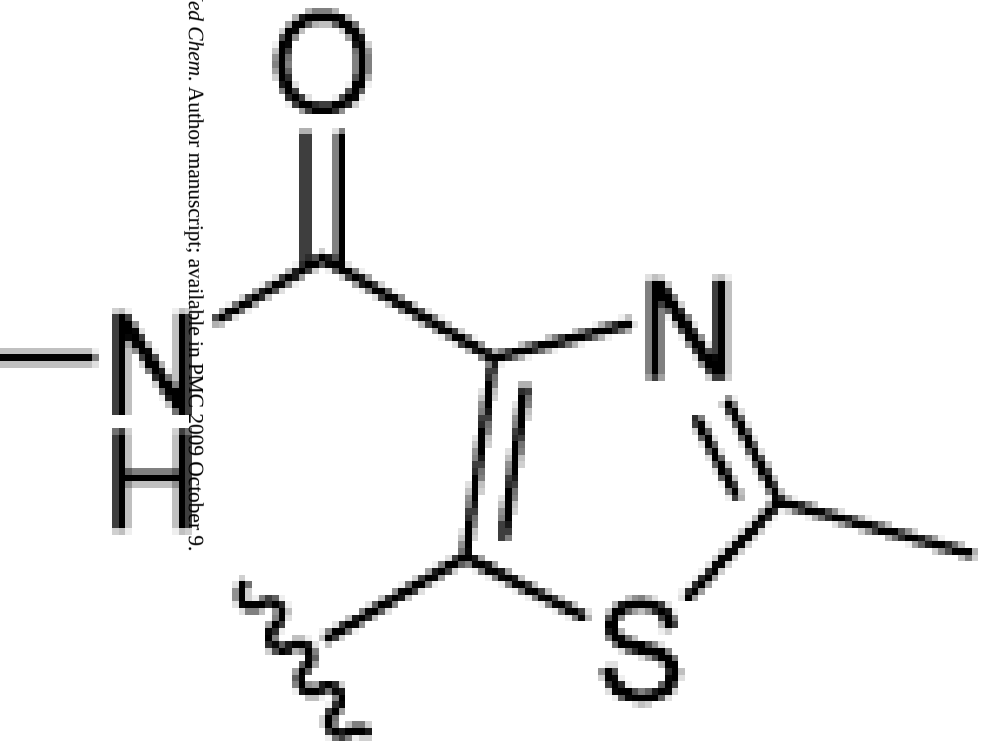

J Med Chem. Author manuscript; available in PMC 2009 October 9.

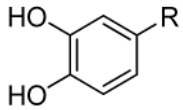

	Inhibition of enzymatic activity, IC_{50}, μM			Inhibition of bacterial growth, IC_{50}, μM [c]			
Co(II)	**Mn(II)**	**Fe(II)**	***E. coli* AS19**	***E. coli* D22**	***B. subtilis***	***B. megaterium***
>100	>100	16.6	235 (198)	98.7 (66)	397 (193)	224 (112)

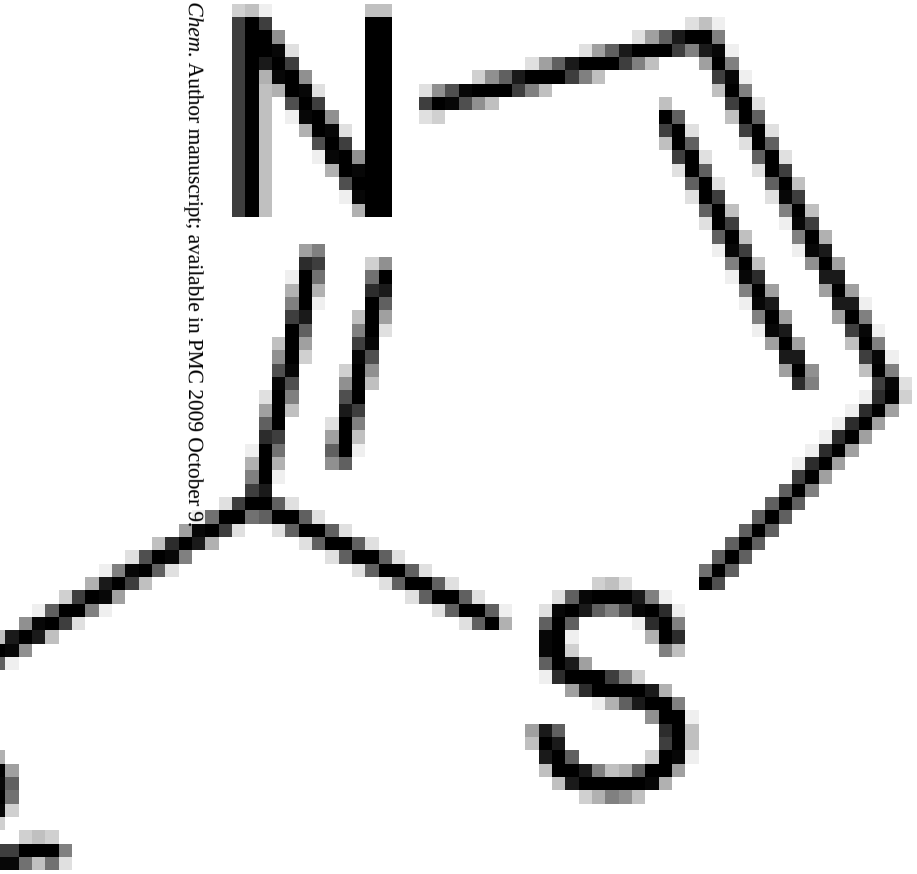

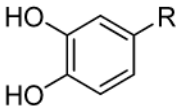

	Inhibition of enzymatic activity, IC_{50}, μM			Inhibition of bacterial growth, IC_{50}, μM [c]			
Co(II)	**Mn(II)**	**Fe(II)**	***E. coli* AS19**	***E. coli* D22**	***B. subtilis***	***B. megaterium***
>100	>100	7.8	116 (113)	254 (151)	109 (56)	54.0 (79)
28.5	34.0	23.8	110 (78)	238 (105)	211 (122)	133 (85)
23.7	15.7	5.1	32.8	4.0 (3)	16.1 (7)	21.2 (9)
51.5	28.0	32.7	87.7 (60)	39.1 (18)	25.1 (10)	26.0 (10)

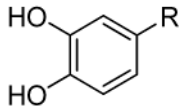

	Inhibition of enzymatic activity, IC_{50}, μM			Inhibition of bacterial growth, IC_{50}, μM [c]			
Co(II)	**Mn(II)**	**Fe(II)**	***E. coli* AS19**	***E. coli* D22**	***B. subtilis***	***B. megaterium***
36.3	30.4	14.8	20.1 (11)	44.2 (15)	14.6 (13)	15.3 (9)

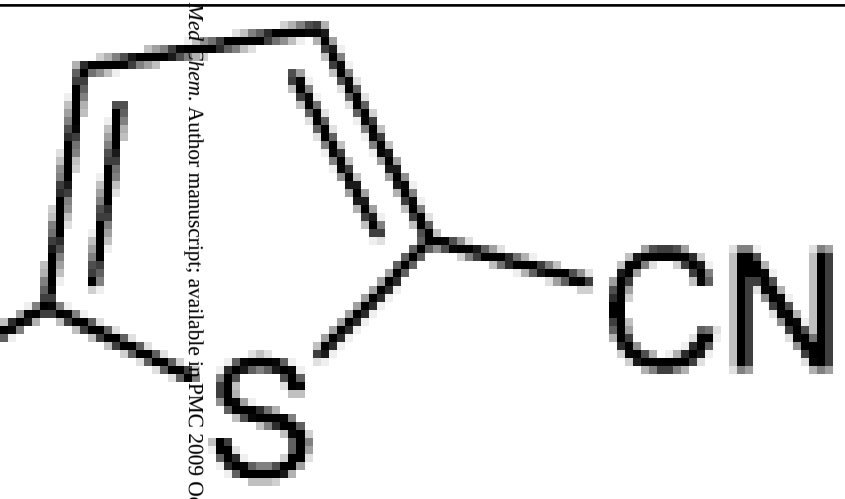

Inhibition of enzymatic activity, IC_{50}, μM				Inhibition of bacterial growth, IC_{50}, μM [c]		
Co(II)	Mn(II)	Fe(II)	*E. coli* AS19	*E. coli* D22	*B. subtilis*	*B. megaterium*
>100	44.8	12.8	15.5 (7)	7.5 (3)	7.1 (2)	6.3 (2)

	Inhibition of enzymatic activity, IC_{50}, μM			Inhibition of bacterial growth, IC_{50}, μM [c]			
	Co(II)	Mn(II)	Fe(II)	*E. coli* AS19	*E. coli* D22	*B. subtilis*	*B. megaterium*
	42.7	23.0	8.0	15.2 (7)	9.0 (3)	22.1 (8)	15.3 (13)

	Inhibition of enzymatic activity, IC_{50}, μM			Inhibition of bacterial growth, IC_{50}, μM [c]		
	Co(II)	Mn(II)	Fe(II)	*E. coli* AS19	*E. coli* D22	*B. subtilis*	*B. megaterium*
	62.6	55.7	12.9	15.4 (5)	11.8 (6)	21.8 (7)	27.8 (11)

Inhibition of enzymatic activity, IC_{50}, μM				Inhibition of bacterial growth, IC_{50}, μM [c]		
Co(II)	Mn(II)	Fe(II)	*E. coli* AS19	*E. coli* D22	*B. subtilis*	*B. megaterium*
100	34.3	14.0	15.5 (4)	43.0 (19)	14.9 (4)	15.5 (6)

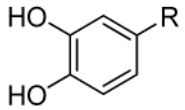

	Inhibition of enzymatic activity, IC_{50}, μM			Inhibition of bacterial growth, IC_{50}, μM [c]			
Co(II)	**Mn(II)**	**Fe(II)**	***E. coli* AS19**	***E. coli* D22**	***B. subtilis***	***B. megaterium***
>100	48.2	9.2	12.4 (5)	13.5 (5)	7.8 (3)	7.6 (3)

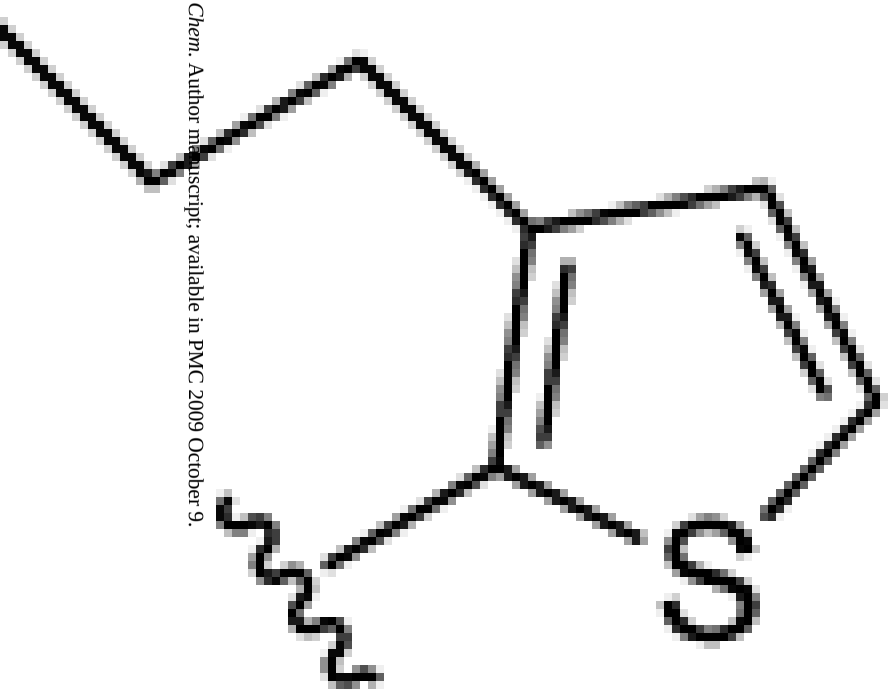

Inhibition of enzymatic activity, IC_{50}, μM				Inhibition of bacterial growth, IC_{50}, μM [c]		
Co(II)	Mn(II)	Fe(II)	*E. coli* AS19	*E. coli* D22	*B. subtilis*	*B. megaterium*
14.0	22.4	7.3	11.3 (5)	86.0 (51)	25.2 (10)	21.1 (14)

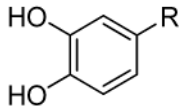

	Inhibition of enzymatic activity, IC_{50}, μM			Inhibition of bacterial growth, IC_{50}, μM [c]			
Co(II)	**Mn(II)**	**Fe(II)**	***E. coli* AS19**	***E. coli* D22**	***B. subtilis***	***B. megaterium***
40.4	27.5	3.8	29.9 (15)	2.0 (2)	15.7 (9)	19.2 (10)

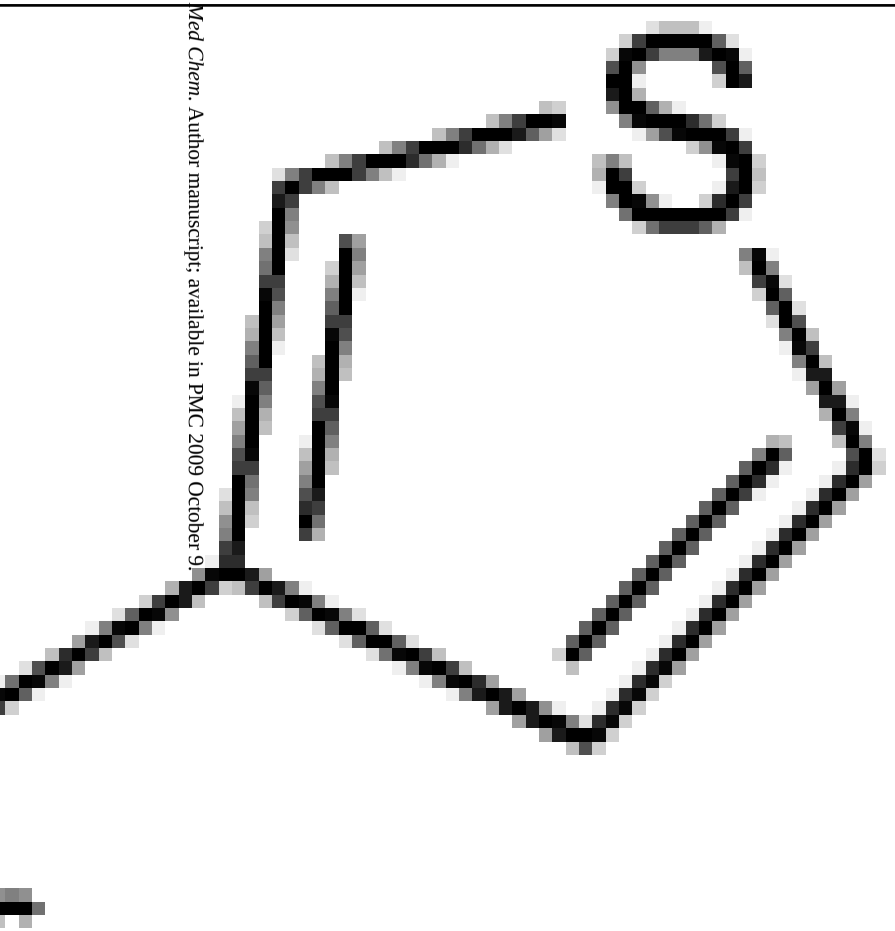

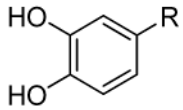

	Inhibition of enzymatic activity, IC_{50}, μM			Inhibition of bacterial growth, IC_{50}, μM [c]			
	Co(II)	**Mn(II)**	**Fe(II)**	***E. coli* AS19**	***E. coli* D22**	***B. subtilis***	***B. megaterium***
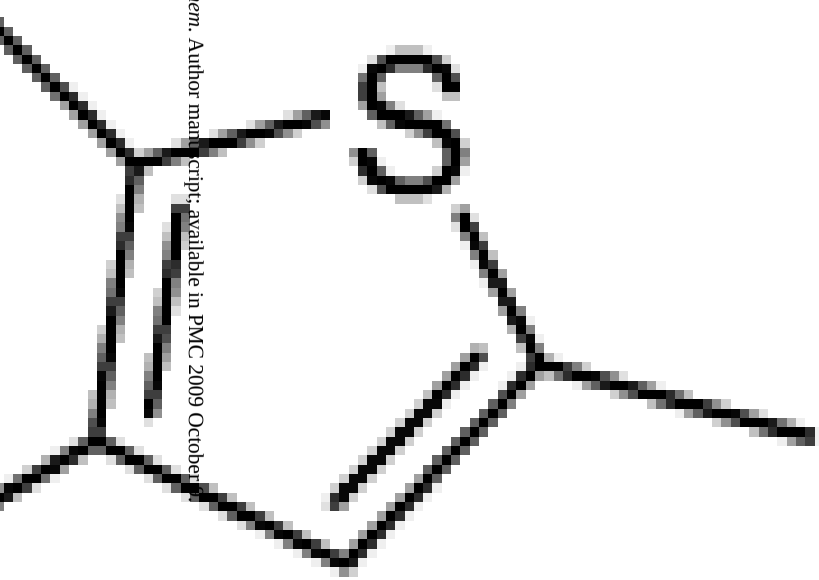	>100	>100	7.4	18.5 (9)	3.7 (4)	16.5 (5)	16.0 (5)
	62.4	48.6	20.2	6.1 (3)	7.3 (2)	6.0 (2)	5.0 (1)

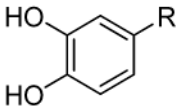

	Inhibition of enzymatic activity, IC_{50}, μM			Inhibition of bacterial growth, IC_{50}, μM [c]			
	Co(II)	**Mn(II)**	**Fe(II)**	***E. coli* AS19**	***E. coli* D22**	***B. subtilis***	***B. megaterium***
	2.4	2.1	3.1	10.8 (5)	7.7 (9)	12.8 (8)	17.5 (10)

values.

ion of *E. coli* AS19 strain, and their IC_{50} values in μM are 95.9, 158, 206, 63.3, 204, 117, and 125, respectively.

/ml.

J Med Chem. Author manuscript; available in PMC 2009 October 9.

Table 2

X-ray data collection and refinement statistics Cell Parameters

Cell Parameters	
space group	$P2_1$
a (Å)	38.5
b (Å)	59.9
c (Å)	54.9
β (deg)	106.5
X-ray Data Collection	
resolution range (Å)	39.5–2.2
collected reflections	47,549
unique reflections	12,282
completeness (%) (last shell)	100 (99.7)
Redundancy (last shell)	3.9 (3.8)
I/σ (I) (last shell)	19.4 (5.4)
R_{merge} (%) (last shell)	7.0 (21.6)
Refinement Statistics	
resolution range (Å)	26.9–2.2
R (%)	19.1
R_{free} (%)	24.4
Rmsd bonds (Å)	0.007
Rmsd angles (deg)	1.065
no. of solvent molecules	139
<B> overall ($Å^2$)	20.4
<B> enzyme ($Å^2$)	20.2
<B> Mn(II) ions ($Å^2$)	19.5
<B> inhibitor ($Å^2$)	32.8
<B> water ($Å^2$)	24.7